Mapping subnational HIV mortality in six Latin American countries with incomplete vital registration systems

KHATAB, Khaled <http://orcid.org/0000-0002-8755-3964>

Supplemental Appendix: Mapping HIV mortality in six Latin American countries with incomplete vital registration systems

Table of Contents

Supplemental Methods

Vital registration completeness

We use a Bayesian hierarchical modelling framework to account for VR systems that vary in completeness by municipality and over time (Figure S1). Our methods expand upon a similar procedure developed in Brazil for estimating life expectancy [1], where a Bayesian framework bypasses a lack of identifiability between the mortality rate and completeness estimate by incorporating an informed prior on the VR completeness. In this analysis, we incorporate information from the GBD [2] on subnational (for Brazil and Mexico) and national VR completeness (for remaining countries) as well as geographic patterns in under-5 VR completeness from past analyses [3] to generate priors on municipality-level VR coverage by two age groups (<15 year-old's and 15+) and year (Figure S3).

In the present analysis, we model different levels of VR completeness in children and adolescents under 15 years (<15) and for adults ages 15 years and over (15+). We model these age groups separately based on the available national VR completeness estimated in GBD and established literature and expert opinion [4]. We do not model VR completeness for adults if GBD completeness estimates for adults exceeds 95% in all years of available VR (Costa Rica and Colombia). Similarly, we do not model under-15 VR completeness if GBD estimates of completeness is greater than 90% in all years of VR data (Costa Rica, Guatemala, Mexico). We therefore model adult completeness in Ecuador, Guatemala, Mexico, and Brazil, and model under-15 completeness in Ecuador, Colombia, and Brazil.

Underlying geographic variation in VR completeness

In order to build priors on geographic variation in VR completeness, we used the underlying geographic variation in completeness in under-5 mortality. We estimated VR completeness in under-5 mortality by comparing the estimated number of under-5 deaths in each municipality from previous analyses [3], where they exist, to the reported number of under-5 deaths from VR data. Previous research produced estimates of under-5 mortality in Ecuador, Colombia, and Guatemala that do not rely on vital registration data and produced 1,000 draws of the number of deaths at the 5 x 5-km level [3]. In these three countries, we used these estimates to generate underlying geographic variation in VR completeness. In Mexico and Brazil, we proceed with a slightly different methodology that leverages state-level estimates of completeness produced by GBD and that is described below.

To generate estimates of underlying geographic variation in VR completeness in Ecuador, Colombia, and Guatemala, we first aggregated estimates of under-5 mortality from the 5 x 5-km grid cell level to each municipality at the draw level by year, such that we derived 1,000 draws of the number of under-5 deaths in each area j and year t. We aggregated these estimates using the same method as our aggregation of covariates and population—we intersected each grid cell with the municipality-level shapefile to determine what fraction of the area of each grid cell fell within each municipality. For cells split across multiple units, we allocated the number of under-5 deaths in proportion to area. These estimates denote the expected number of deaths in the under-5 age group used to inform the denominator for our initial VR completeness estimates π_j^*.

We use the number of reported VR deaths in each area for children under 5 as the numerator for our initial VR completeness estimates π_j^*. Due to stochastic variation from year to year in the total number of deaths by area, especially in areas with low child populations, we aggregated VR deaths over all reported years to smooth the number of deaths over time. Nonetheless, after combining child VR deaths across all years in a given area, in some countries there are still areas that report zero deaths. Given that we do not believe completeness is zero in these areas and this likely represents stochastic noise, we used a simple spatial smoothing model to derive more robust estimates of reported under-5 deaths. The spatial smoothing model is outlined below:

$$d_j \sim \text{Poisson}\left(E_j \cdot e^{\beta_0 + s_j + \epsilon_j}\right)$$

$$\epsilon_j \sim \text{N}(0,\ \sigma_\varepsilon^2)$$

$$S_j \sim \text{ICAR}(0,\ \sigma_S^2)$$

Where d_j denoted under-5 deaths in a municipality across all years of available VR data, E_j represented the under-5 population summed over all years of available VR data, and $e^{\beta_0 + s_j + \epsilon_j}$ represented an estimate of the underlying mortality rate—a linear combination in log-space of an intercept β_0, spatially structured random effect S_j and the unstructured random effect ϵ_j. The spatially structured random effect S_j is an intrinsic conditional autoregressive model (ICAR) model [6]**.** The model was fit in R-INLA [5] using a variation of the Besag, York and Mollié (BYM) model [6] to “borrow strength” from the geographic pattern in reported VR deaths while still allowing for non-spatially structured variation. We used first-order queen contiguity of the spatial units to form the graph for the spatial model. We chose this model over the classic BYM model because it parameterizes the relationship between the spatially structured random effect S_j and the unstructured random effect ϵ_j in terms of two hyperparameters: τ which is the marginal precision and φ which is the portion of the marginal variance described by the spatially structured random effect, which improves the interpretability of the hyperparameters. We used the uninformative default penalized complexity priors [6, 7] available in INLA for these hyperparameters:

$$\varphi = PC(0.5, 0.5)$$

$$\tau = PC(1, 0.01)$$

In the first case, this prior indicates a 50% probability that 50% or more of the variation is spatially autocorrelated. In the second, this prior indicates a 1% chance that the log precision is less than 1. After fitting the model, we calculate the smoothed number of VR under-5 deaths by using the posterior mean estimate of the mortality rate for each area j and multiplying by the sum of the under-5 population over all years. We produce 1,000 draws (i) of the underlying completeness π^* for each area j:

$$\pi^*_{j,i} = {\text{VR deaths}_\text{j}} \Big/ {U5M\ death\text{s}_{j,i}}$$

There are certain areas where $VR\ death\text{h}_j > U5M\ death\text{s}_{j,i}$ and underlying completeness estimates are above 1. Given that we have no reason to believe certain areas are over-reporting deaths, we truncated completeness to either the 99$^{\text{th}}$ percentile of completeness draws in that municipality or 0.99, whichever is greater.

Calibrating to national VR completeness by age group

The methods outlined above produced estimates of subnational geographic variation in VR completeness by municipality in Ecuador, Colombia, and Guatemala, but this variation is not specific to year or age group. We proceed with two different frameworks, one for adult VR completeness estimates and one for under-15 completeness estimates. For both under-15 and adults, we rescale the municipality-level completeness estimates such that the death-weighted aggregation matches the GBD national VR completeness estimates.

For national adult VR completeness, GBD produces 1,000 draws (i) of completeness for each country and year t, $\Pi_{t,i}$. We rescale our initial estimates of municipality-level VR completeness, $\pi^*_{j,i}$, at the draw level such that the expected number of true deaths among adults in each area j and year t, calculated as the number of reported adult VR deaths $d^{adult}_{j,t}$ divided by completeness $\pi^*_{j,i}$ is equal to the total number of expected national deaths by year D^{adult}_t. The total number of expected national deaths D^{adult}_t is calculated as the sum of all municipality-level adult VR deaths $D^{adult}_t = \sum_j d^{adult}_{j,t}$ divided by the national GBD completeness $\Pi_{t,i}$. We rescale the municipality-level completeness estimates at the draw level in logit space to ensure completeness remains between zero and one while scaling the expected number of deaths to GBD by adding an adjustment factor $c^{adult}_{t,i}$ as represented in the equation below for each country:

$$\sum_j \left(d^{adult}_{j,t} \Big/ \text{logit}^{-1}(\text{logit}(\pi^*_{j,i} + c^{adult}_{t,i})) \right) = D^{adult}_t \Big/ \Pi_{t,i}$$

$$\sum_j d^{adult}_{j,t} = D^{adult}_t$$

We calculated and applied 1,000 draws of the adjustment factor $c^{adult}_{t,i}$ to each municipality-draw of the initial completeness in year t to produce 1,000 draws of initial completeness for each municipality and year: $\pi^{\text{adult}}_{j,t,i} = \text{logit}^{-1}(\text{logit}(\pi^*_{j,i} + c^{adult}_{t,i}))$.

For under-15 VR completeness, we undertook a different approach given that GBD does not produce draws of child completeness. In this case, for each country and year t we pulled 1,000 draws of the estimated under-15 all-cause deaths from the GBD, $D^{under15}_t$. We then rescaled the expected number under-15 deaths in municipality j and year t to equal to the estimated number of under-15 deaths from GBD by applying an adjustment factor $c^{under15}_{t,i}$ to each municipality in logit space:

$$\sum_j d^{under15}_{j,t} \Big/ \text{logit}^{-1}(\text{logit}(\pi^*_{j,i} + c^{under15}_{t,i})) = D^{under15}_{t,i}$$

We calculated and applied 1,000 draws of the adjustment factor $c_{t,i}^{under15}$ to each municipality-draw of the initial completeness in year t to produce 1,000 draws of initial completeness for each municipality and year: $\pi_{j,t,i}^{\text{under15}} = \text{logit}^{-1}(\text{logit}(\pi^{*}_{j,i} + c_{t,i}^{under15`}))$.

Completeness draws for Brazil and Mexico

For Brazil and Mexico, we leverage state-level estimates of VR completeness for adults and children produced by GBD [2]. For state-level adult VR completeness, GBD produces 1,000 draws (i) of completeness for each state J and year t, $\Pi_{\text{J,t},i}$.These estimates of adult completeness at the state level are modelled directly in our small area estimation framework, where each municipality that nests within a state is assumed to follow the same prior and contributes to the same posterior level of VR completeness.

For under-15 completeness in Brazil, given that GBD does not produce draw-level completeness, we extracted 1,000 draws of estimated under-15 all-cause deaths for each state J and year t: $D_{J,t,i}$. We then calculate draws of completeness by taking the ratio of the reported all-cause deaths for each state J and year t from VR data and $D_{J,t,i}$:

$$\pi_{J,t,i}^{\text{under15}} = {VR\ deaths_{J,t}}\Big/{D_{J,t,i}}$$

In a small number of state draws, completeness estimates are greater than 1 and these are truncated to 0.99. These estimates of under-15 completeness at the state level are modelled directly in our small area estimation framework, where each municipality that nests within a state inherits the same prior and contributes to the posterior for VR completeness.

Prior specification

The processes outlined above generate draws of both adult and under-15 completeness for each municipality (Ecuador, Colombia, Guatemala) or state (Brazil and Mexico) by year. To include these informed priors in our modelling framework, we characterized the distribution by fitting to a logit-normal distribution using maximum likelihood estimation. For area-municipality-years where all draws were truncated at 0.99, we fit the model with a mean of 0.99 and a standard deviation of 0.01 in logit space.

Statistical model

We fit the following hierarchical generalized linear model for VR data, building on a model developed in prior modelling studies [8, 9]

$$D_{j,t,a} \sim \text{Poisson}\left(m_{j,t,a} \cdot \pi_{k,t,a^*} \cdot P_{j,t,a}\right)$$

$$\gamma_{1,a,t} \sim \text{LCAR: LCAR}\left(\sigma_1^2, \rho_{1,A}, \rho_{1,T}\right)$$

$$\gamma_{2,j} \sim \text{LCAR}(\sigma_2^2, \rho_2)$$

$$\gamma_{3,j} \sim \text{LCAR}(\sigma_3^2, \rho_3)$$

$$\gamma_{4,j} \sim \text{LCAR}(\sigma_4^2, \rho_4)$$

$$\gamma_{5,j,t} \sim \text{N}(0, \sigma_5^2)$$

$$\gamma_{6,j,a} \sim \text{N}(0, \sigma_6^2)$$

$$1/_{\sigma_i^2} \sim \text{Gamma}(1, 1000) \text{ for } i \in 1, 2, 3, 4, 5, 6$$

$$\text{logit}(\rho_i) \sim \text{Normal}(0, 1.5) \text{ for } i \in 1A, 1T, 2, 3, 4$$

where $D_{j,t,a}$ represents the number of HIV deaths in municipality *j*, year *t,* and age group *a; $m_{j,t,a}$* is the mortality rate in municipality *j*, year *t,* and age group *a*; π_{k,t,a^*} is the VR completeness in municipality (Colombia, Ecuador, and Guatemala) or state (Brazil and Mexico) *j*, year *t,* and completeness age group a^* (<15, 15+); $P_{j,t,a}$ is the population in municipality *j*, year *t,* and age group *a*; β_0 is the intercept; $\beta_1 \cdot X_j$ is the vector of covariates and associated regression coefficients; $\gamma_{1,a,t}$ describes the overall age-time pattern; $\gamma_{2,j}$ describes spatial patterns that persist over age and time, $\gamma_{3,j} \cdot \text{t}$ describes area-specific deviations from the overall time pattern; $\gamma_{4,j} \cdot \text{a}$ describes area-specific deviations from the overall age pattern; $\gamma_{5,j,t}$ and $\gamma_{6,j,a}$ allow for area-specific non-linear deviations from the overall time and age patterns, respectively.

VR completeness is incorporated into the data generating model, and logit-normal priors on π_{k,t,a^*} fit on empirical data as described above allow the model to distinguish between mortality rate $m_{j,t,a}$ and the VR completeness. Random effects $\gamma_{1,a,t}, \gamma_{2,j}, \gamma_{3,j}, \gamma_{4,j}$ were assigned a Leroux conditional autoregressive prior (LCAR) [10]. The full conditional distribution can be described by:

$$\gamma_i|\gamma_{k\sim i},\sigma^2,\rho \sim \text{Normal}\left(\frac{\rho\sum_{k\sim i}\gamma_k}{n_i\cdot\rho+1-\rho},\frac{\sigma^2}{n_i\cdot\rho+1-\rho}\right)$$

where: $k \sim i$ denotes the set of i's "neighbors" (for spatial terms, municipalities that share a border; for temporal/age terms, adjacent years/age groups); n_j is the number of neighbors in $k \sim i$; σ^2 is the variance parameter; and ρ is the correlation parameter. These random effects allow for additional variation across space, time, and age that is not explained by the covariates. For each of the random effects, the variance (σ^2) denotes the amount of variation, while the correlation (ρ) determines how much smoothing takes place, ρ ranged 0 to 1 with higher values indicating greater spatial smoothness. We assigned Gamma(0, 1000) hyperpriors for the precision of each random effect and Normal(0, 1.5) hyperpriors for the logit-transform of the correlation parameters. The random effects $\gamma_{5,j,t}$ and $\gamma_{6,j,a}$ were assumed to follow independent mean-zero normal distributions.

We model γ_1 as an interaction between two conditional autoregressive (LCAR) distributions as defined above for age and time, respectively. This was specified according to the procedure described by Knorr-Held (i.e., a 'Type IV' interaction) [11]. This specification allows for smoothing over age group and time simultaneously, such that the level for a given age group and year is informed both by first-order neighbors (i.e., adjacent years in the same age group and adjacent age groups in the same year) as well as second order neighbors (i.e., adjacent years in adjacent age groups). For this distribution there are three hyperparameters: σ^2, which control the overall amount of variation, and $\rho_{1,A}$ and $\rho_{1,T}$ which control the smoothness over age and time, respectively.

References

1. Schmertmann CP, Gonzaga MR. Bayesian Estimation of Age-Specific Mortality and Life Expectancy for Small Areas With Defective Vital Records. Demography. 2018;55:1363–88.

2. Roth GA, Abate D, Abate KH, Abay SM, Abbafati C, Abbasi N, et al. Global, regional, and national age-sex-specific mortality for 282 causes of death in 195 countries and territories, 1980–2017: a systematic analysis for the Global Burden of Disease Study 2017. The Lancet. 2018;392:1736–88.

3. Burstein R, Henry N, Collison M, Marczak L, Sligar A, Watson S, et al. Mapping 123 million neonatal, infant and child deaths between 2000 and 2017. Nature. 2019;574:353–358.

4. Målqvist M, Eriksson L, Nga N, Fagerland L, Hoa D, Ewald U, et al. Unreported births and deaths, a severe obstacle for improved neonatal survival in low-income countries; a population based study. BMC international health and human rights. 2008;8:4.

5. The R-INLA project. R-INLA. 2019. http://www.r-inla.org/. Accessed 25 Jul 2019.

6. Riebler A, Sørbye S, Simpson D, Rue H. An intuitive Bayesian spatial model for disease mapping that accounts for scaling. 2015.

7. Fuglstad G-A, Simpson D, Lindgren F, Rue H. Constructing Priors that Penalize the Complexity of Gaussian Random Fields. Journal of the American Statistical Association. 2018.

8. Ross J, Henry N, Dwyer-Lindgren L, Lobo A, Marinho de Souza MDF, Biehl M, et al. Progress toward eliminating TB and HIV deaths in Brazil, 2001-2015: A spatial assessment. BMC Medicine. 2018;16.

9. Dwyer-Lindgren L, Bertozzi-Villa A, Stubbs RW, Morozoff C, Kutz MJ, Huynh C, et al. US County-Level Trends in Mortality Rates for Major Causes of Death, 1980-2014. JAMA. 2016;316:2385–401.

10. Leroux BG, Lei X, Breslow N. Estimation of Disease Rates in Small Areas: A new Mixed Model for Spatial Dependence. In: Halloran ME, Berry D, editors. Statistical Models in Epidemiology, the Environment, and Clinical Trials. New York, NY: Springer; 2000. p. 179–91.

11. Knorr-Held L. Bayesian modelling of inseparable space-time variation in disease risk. Stat Med. 2000;19:2555–67.

12. Kristensen K, Nielsen A, Berg CW, Skaug H, Bell BM. TMB: Automatic Differentiation and Laplace Approximation. Journal of Statistical Software. 2016;70:1–21.

13. R Core Team. R: a language and environment for statistical computing. Vienna, Austria: Foundation for Statistical Computing; 2015.

Compliance with the Guidelines for Accurate and Transparent Health Estimates Reporting (GATHER)

Item #	Checklist item	Description of Compliance
Objectives and funding		
1	Define the indicator(s), populations (including age, sex, and geographical entities), and time period(s) for which estimates were made.	Manuscript: Background, Methods
2	List the funding sources for the work.	Manuscript: Declarations (Funding)
Data Inputs		
For all data inputs from multiple sources that are synthesised as part of the study:		
3	Describe how the data were identified and how the data were accessed.	Manuscript: Methods
4	Specify the inclusion and exclusion criteria. Identify all ad-hoc exclusions.	Manuscript: Methods
5	Provide information on all included data sources and their main characteristics. For each data source used, report reference information or contact name/institution, population represented, data collection method, year(s) of data collection, sex and age range, diagnostic criteria or measurement method, and sample size, as relevant.	Supplemental Tables S1 and S2
6	Identify and describe any categories of input data that have potentially important biases (e.g., based on characteristics listed in item 5).	Manuscript: Discussion (Limitations)
For data inputs that contribute to the analysis but were not synthesised as part of the study:		
7	Describe and give sources for any other data inputs.	Manuscript: Methods; Supplemental Table S3
For all data inputs:		
8	Provide all data inputs in a file format from which data can be efficiently extracted (e.g., a spreadsheet rather than a PDF), including all relevant meta-data listed in item 5. For any data inputs that cannot be shared because of ethical or legal reasons, such as third-party ownership, provide a contact name or the name of the institution that retains the right to the data.	Available through GHDx: http://ghdx.healthdata.org/record/ihme-data/latin-america-hiv-mortality-estimates-2000-2017
Data analysis		
9	Provide a conceptual overview of the data analysis method. A diagram may be helpful.	Manuscript: Methods; Figure S1-S3

10	Provide a detailed description of all steps of the analysis, including mathematical formulae. This description should cover, as relevant, data cleaning, data pre-processing, data adjustments and weighting of data sources, and mathematical or statistical model(s).	Manuscript: Methods
11	Describe how candidate models were evaluated and how the final model(s) were selected.	Manuscript: Methods
12	Provide the results of an evaluation of model performance, if done, as well as the results of any relevant sensitivity analysis.	Manuscript: Methods
13	Describe methods for calculating uncertainty of the estimates. State which sources of uncertainty were, and were not, accounted for in the uncertainty analysis.	Manuscript: Methods
14	State how analytic or statistical source code used to generate estimates can be accessed.	Available through GHDx: http://ghdx.healthdata.org/record/ihme-data/latin-america-hiv-mortality-estimates-2000-2017
Results and Discussion		
15	Provide published estimates in a file format from which data can be efficiently extracted.	Available through GHDx: http://ghdx.healthdata.org/record/ihme-data/latin-america-hiv-mortality-estimates-2000-2017
16	Report a quantitative measure of the uncertainty of the estimates (e.g., uncertainty intervals).	Manuscript: Results
17	Interpret results in light of existing evidence. If updating a previous set of estimates, describe the reasons for changes in estimates.	Manuscript: Discussion
18	Discuss limitations of the estimates. Include a discussion of any modelling assumptions or data limitations that affect interpretation of the estimates.	Manuscript: Discussion

Supplemental Figures

Figure S1: Analytical process overview

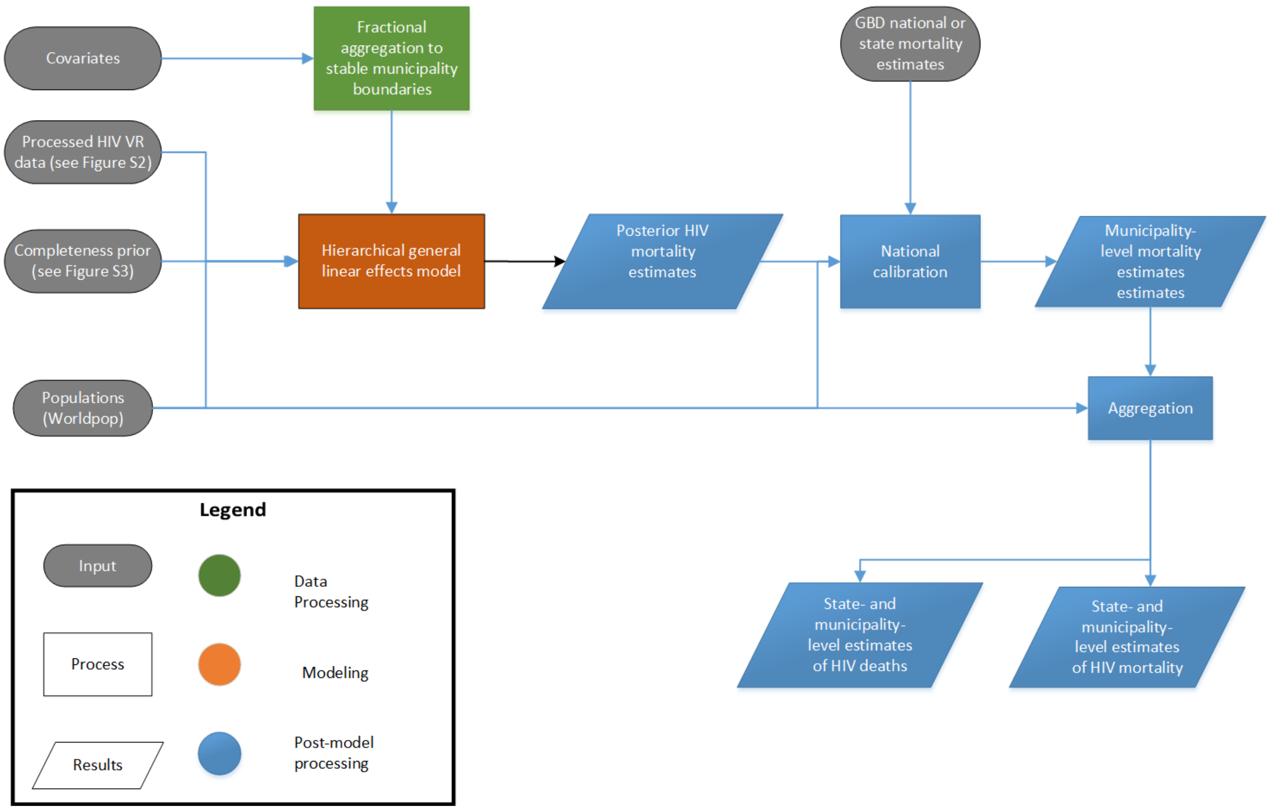

Figure S1: Analytical process overview. The process used to produce HIV mortality estimates by age, sex, year, and municipality involved three main parts. In the data processing steps (green) data were identified, extracted and prepared for use in the HIV mortality model. In the modeling phase (orange) we used data and covariates in a hierarchical linear effects model. In the post-model processing (blue) we calibrated mortality estimates to national GBD 2017 estimates, aggregated mortality estimates to the state level, and calculated the number of HIV deaths.

Figure S2: Analytical process for VR data

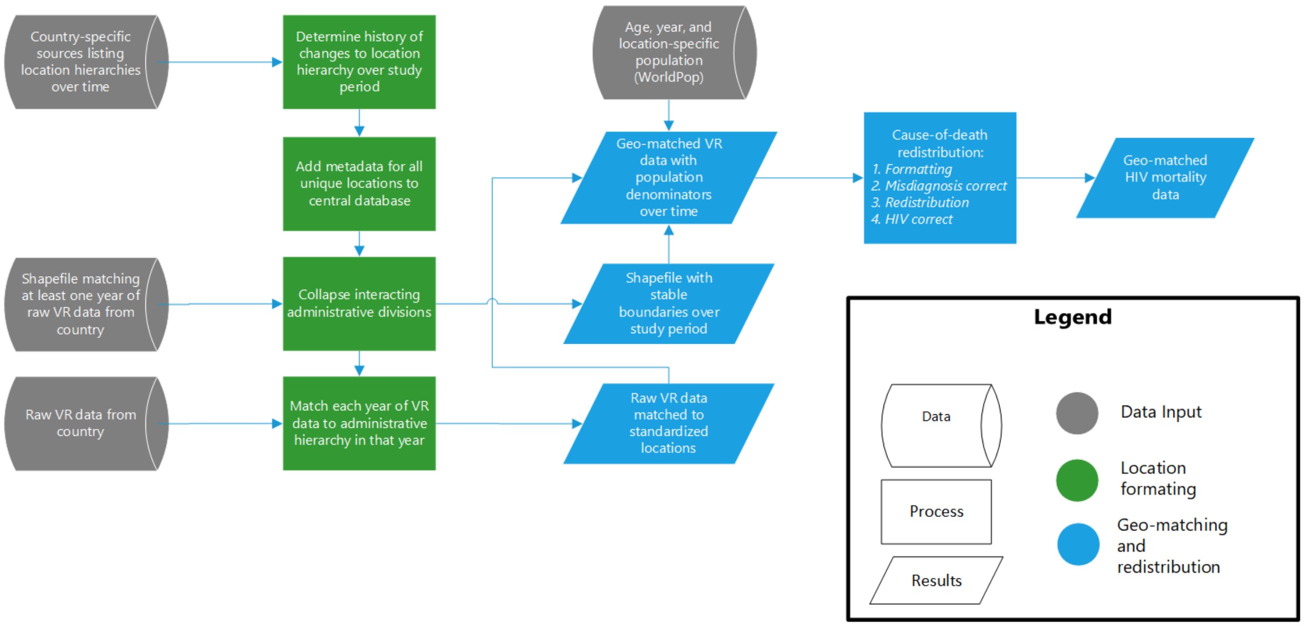

Figure S2: Analytical process for VR data. The process used to process VR data for our analysis consisted of three main parts. In the data input steps (grey) country specific shapefiles and location hierarchies were acquired to match to raw VR data. In the location formatting steps (green) we matched VR data to stable areas over the years of study. In the geo-matching and redistribution phase (blue) we produced a stable shapefile over the years of study and raw VR data was processed using cause of death redistribution as outlined in GBD 2017. At the end of this process, we produced HIV mortality data matched to stable municipalities within each country.

Figure S3: Analytical process for VR completeness priors

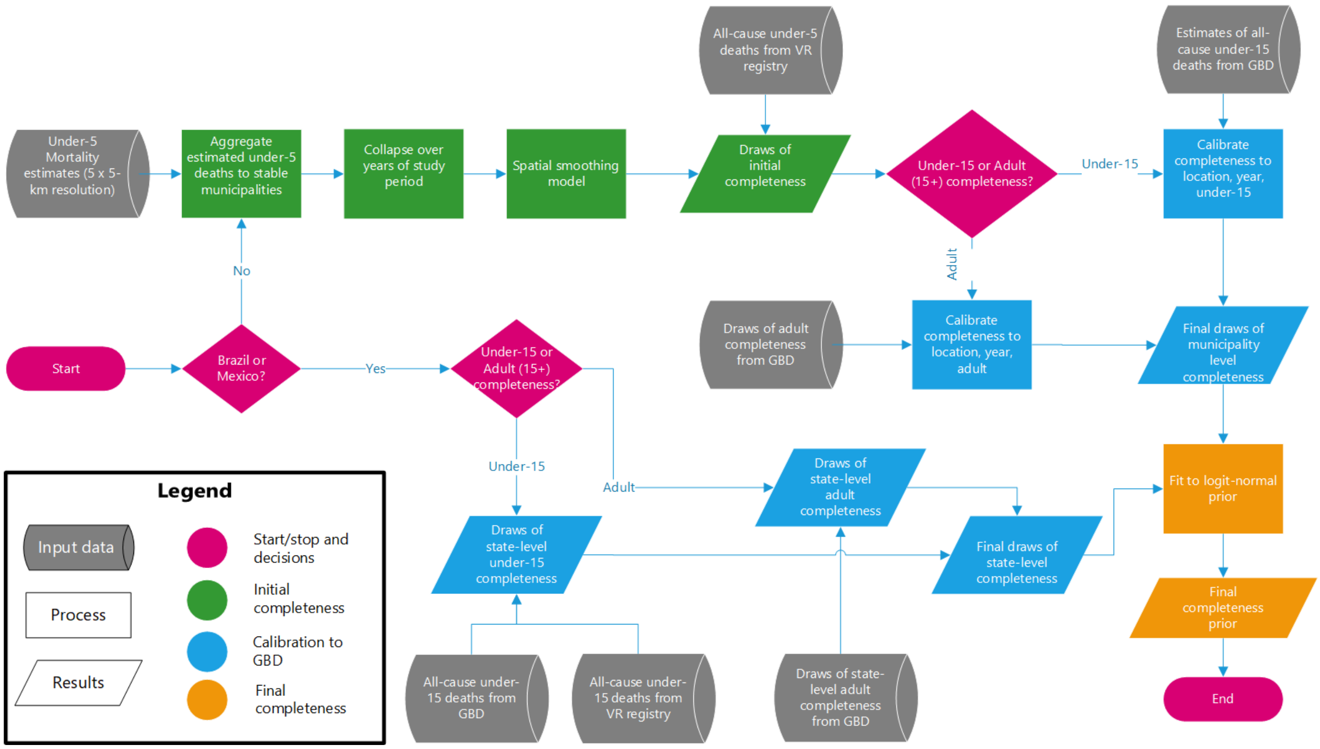

Figure S3: Analytical process overview for VR completeness priors. The process used to process VR data for our analysis consisted of three main parts. In the initial completeness steps (green) for Colombia, Ecuador, and Guatemala, draws of initial completeness were produced using under-5 mortality estimates. In the calibration to GBD steps (blue) state- or municipality-level initial completeness estimates were calibrated to GBD 2017 using draws of national adult completeness or under-15 national deaths. In the final completeness steps (orange) a logit-normal prior was fit to draws of completeness to generate a final completeness prior used in the modeling process.

Figure S4: Model alignment with GBD, Brazil

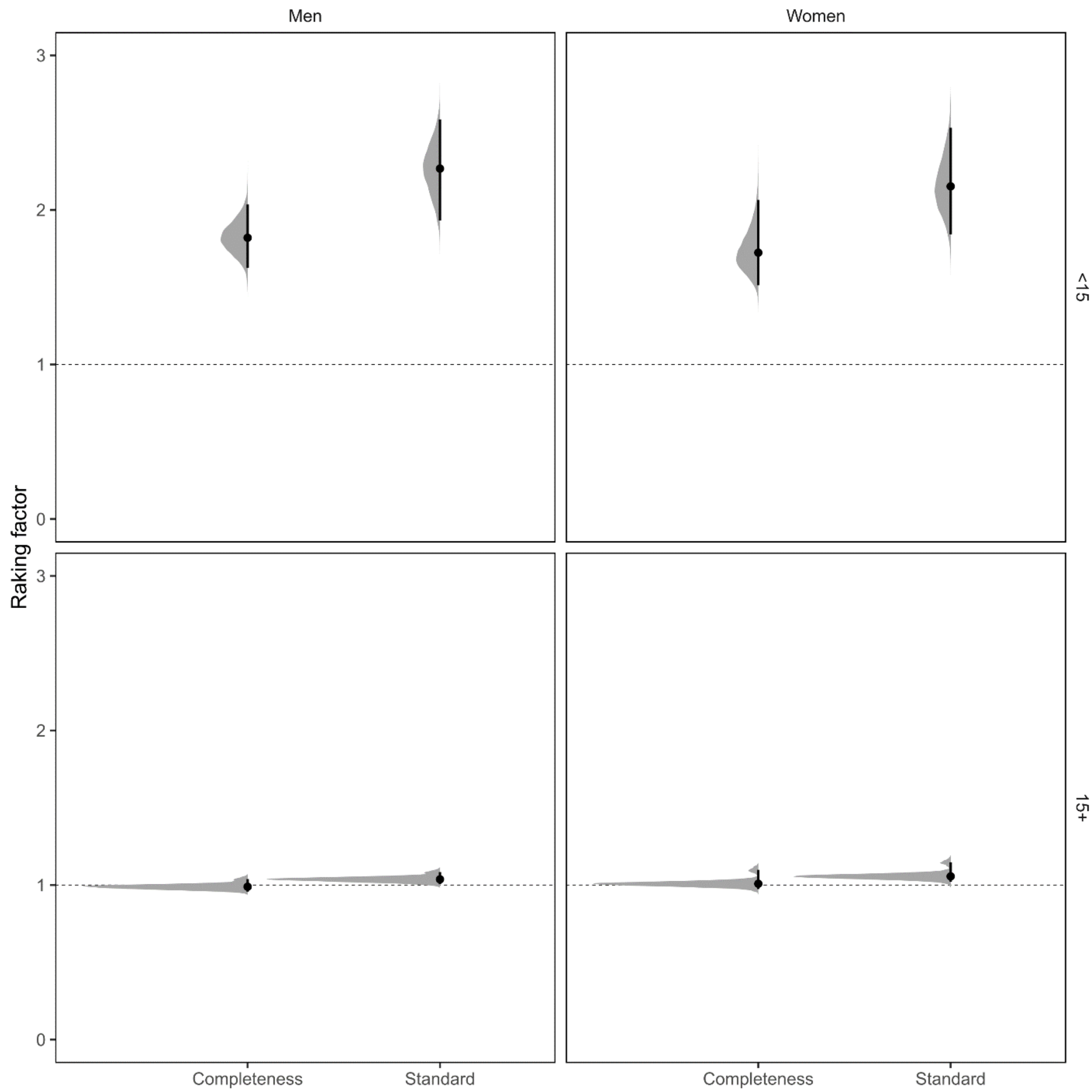

Figure S4: Model alignment with GBD, Brazil. Comparison of the annual ratio of national HIV mortality from GBD and 1,000 draws of annual national HIV mortality in children under-15 (<15) and adults (15+) by sex across the entire range of study (2000 to 2017). The model used in the analysis that includes prior completeness π_{k,t,a^*} ('Completeness') is shown compared to a model without any prior information on completeness ('Standard'). Each point represents the median of the draws of the raking factor, the bar represents 2.5th and 97.5th quantile of the draws, and the density curve represents the relative frequency of the draws. A raking factor closer to 1 (dotted line) indicates better alignment between model results and GBD estimates.

Figure S5: Model alignment with GBD, Colombia

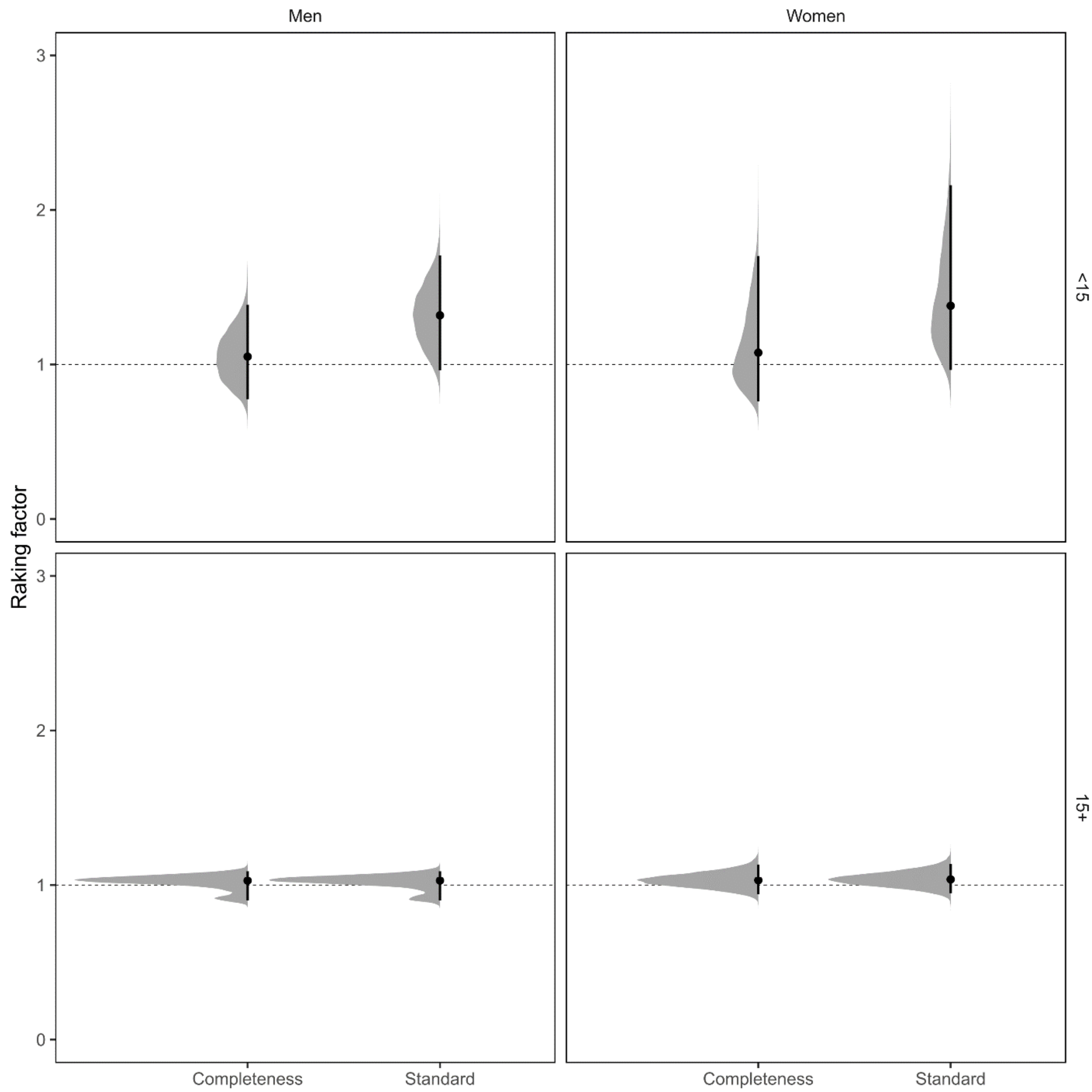

Figure S5: Model alignment with GBD, Colombia. Comparison of the annual ratio of national HIV mortality from GBD and 1,000 draws of annual national HIV mortality in children under-15 (<15) and adults (15+) by sex across the entire range of study (2000 to 2017). The model used in the analysis that includes prior completeness π_{k,t,a^*} ('Completeness') is shown compared to a model without any prior information on completeness ('Standard'). Each point represents the median of the draws of the raking factor, the bar represents 2.5th and 97.5th quantile of the draws, and the density curve represents the relative frequency of the draws. A raking factor closer to 1 (dotted line) indicates better alignment between model results and GBD estimates.

Figure S6: Model alignment with GBD, Costa Rica

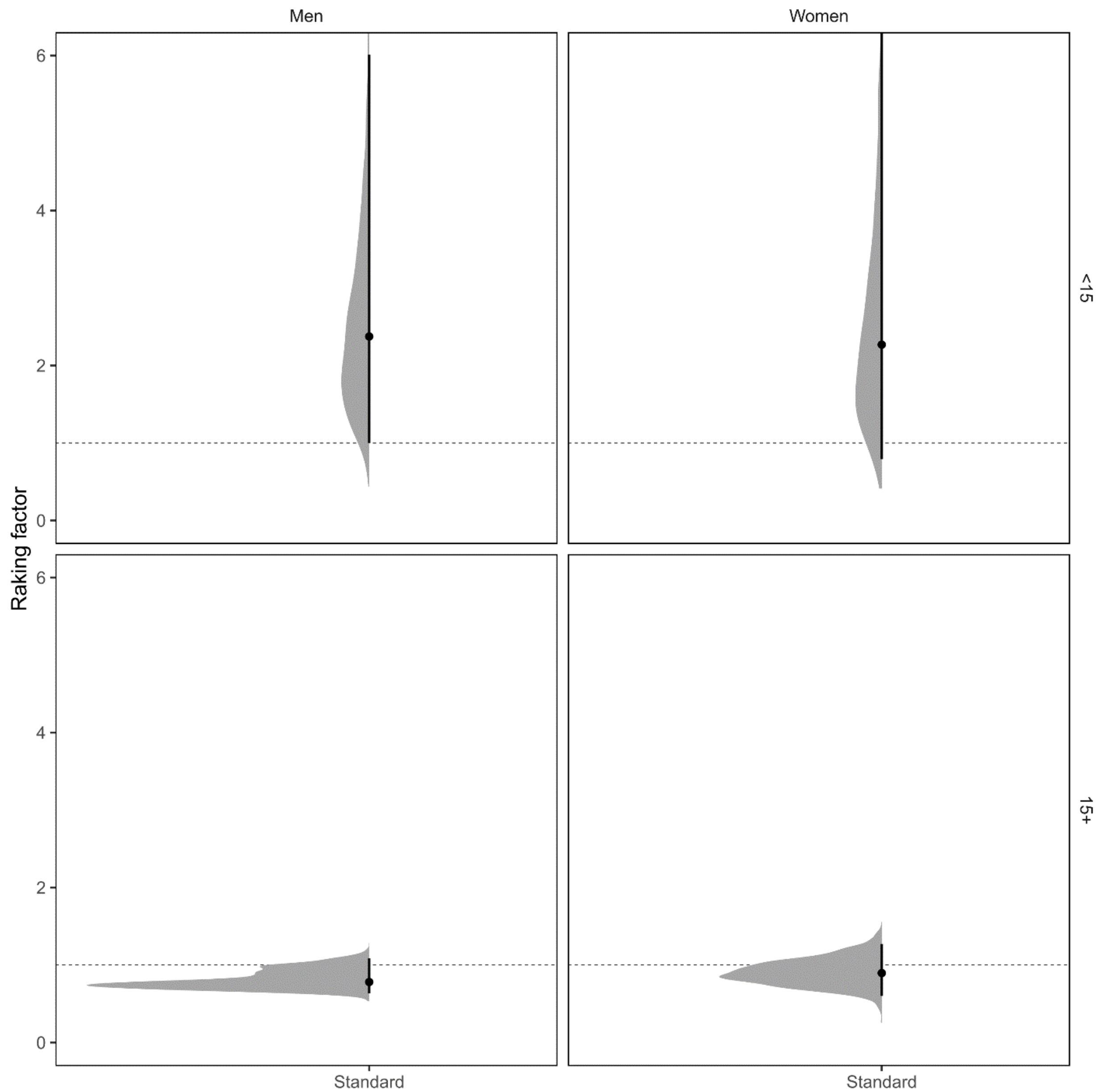

Figure S6: Model alignment with GBD, Costa Rica. Comparison of the annual ratio of national HIV mortality from GBD and 1,000 draws of annual national HIV mortality in children under-15 (<15) and adults (15+) by sex across the entire range of the study (2014 to 2016). We do not model prior completeness for Costa Rica, and we show the final model without any prior information on completeness ('Standard'). Each point represents the median of the draws of the raking factor, the bar represents 2.5th and 97.5th quantile of the draws, and the density curve represents the relative frequency of the draws. A raking factor closer to 1 (dotted line) indicates better alignment between model results and GBD estimates.

Figure S7: Model alignment with GBD, Ecuador

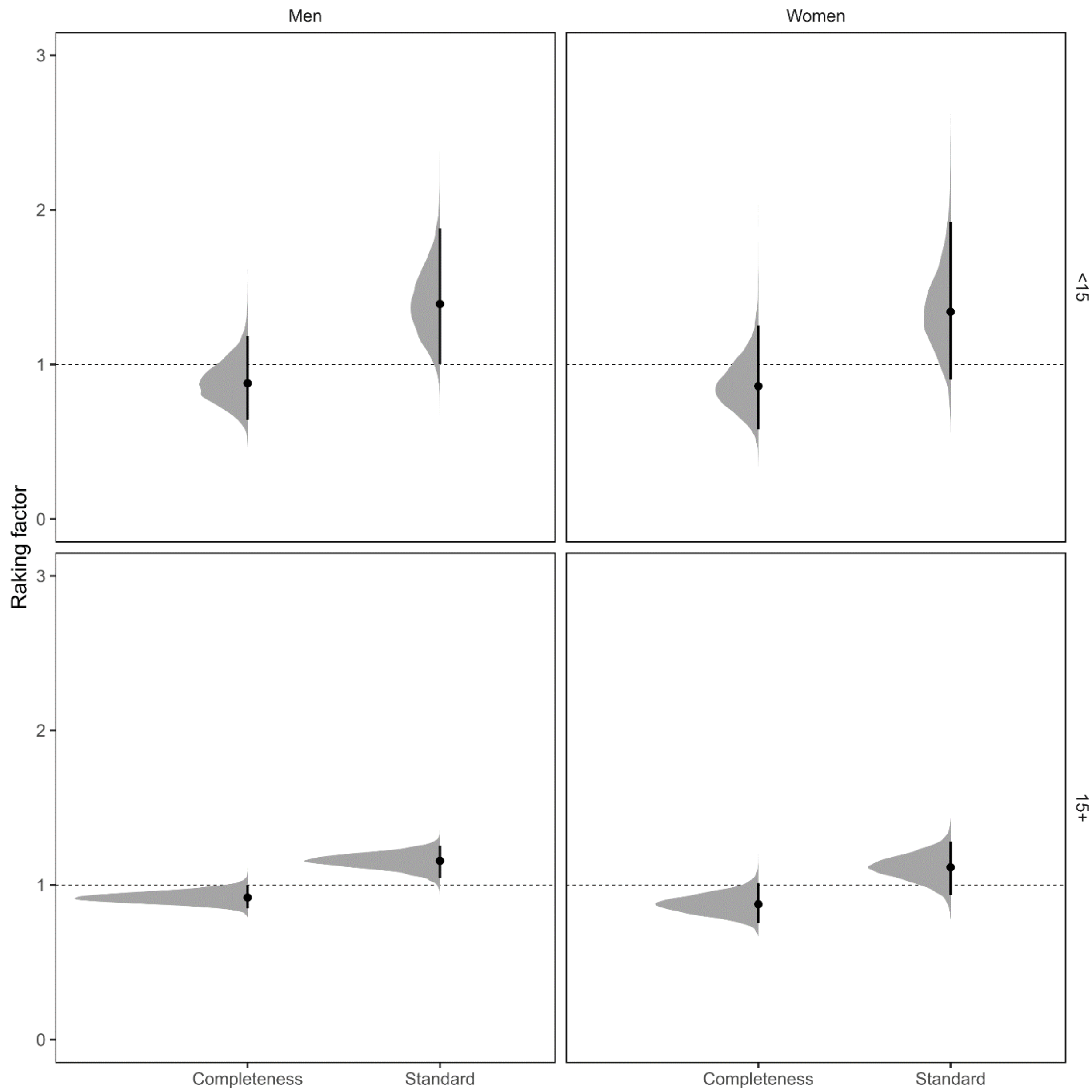

Figure S7: Model alignment with GBD, Ecuador. Comparison of the annual ratio of national HIV mortality from GBD and 1,000 draws of annual national HIV mortality in children under-15 (<15) and adults (15+) by sex across the entire range of study (2004 to 2014). The model used in the analysis that includes prior completeness π_{k,t,a^*} ('Completeness') is shown compared to a model without any prior information on completeness ('Standard'). Each point represents the median of the draws of the raking factor, the bar represents 2.5th and 97.5th quantile of the draws, and the density curve represents the relative frequency of the draws. A raking factor closer to 1 (dotted line) indicates better alignment between model results and GBD estimates.

Figure S8: Model alignment with GBD, Guatemala

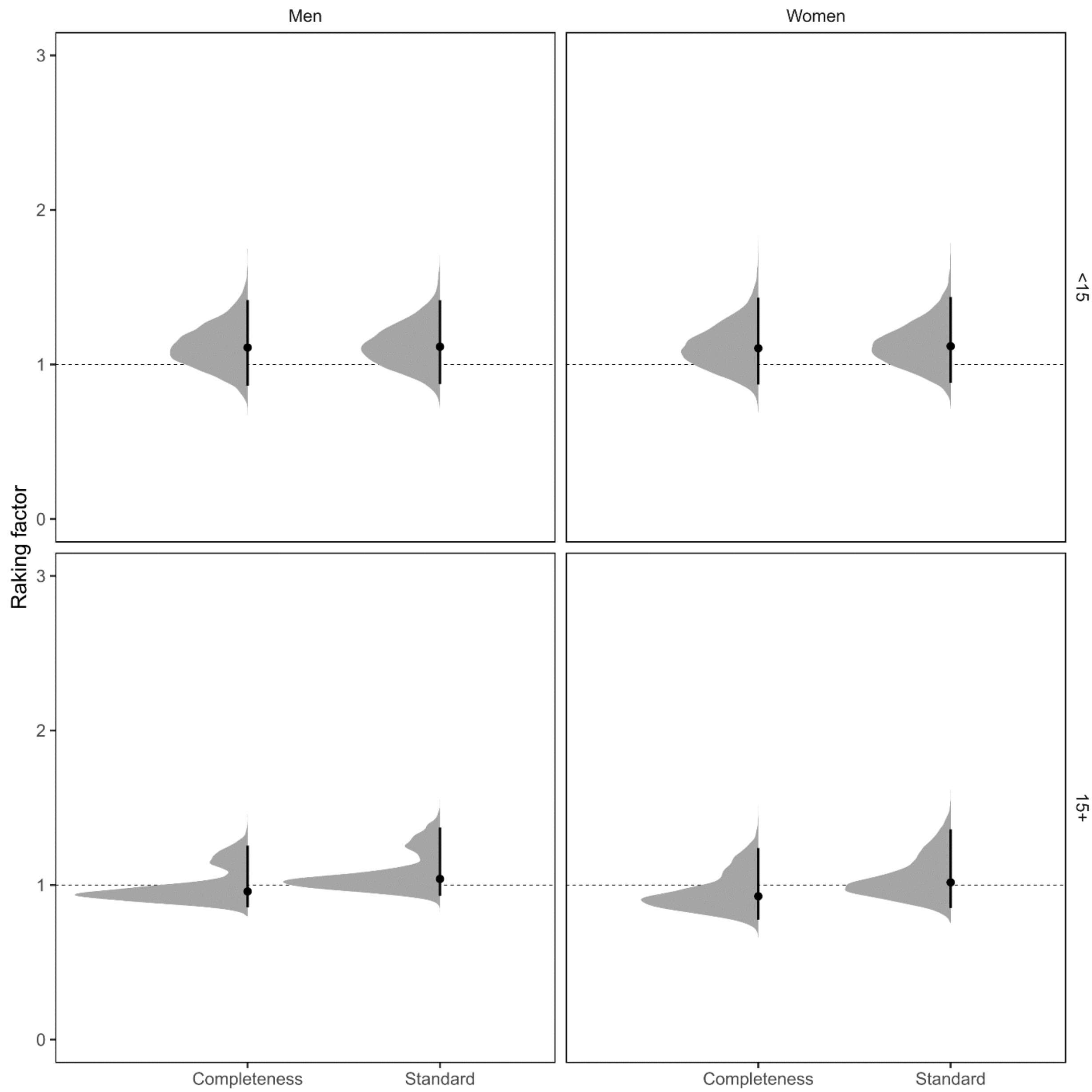

Figure S8: Model alignment with GBD, Guatemala. Comparison of the annual ratio of national HIV mortality from GBD and 1,000 draws of annual national HIV mortality in children under-15 (<15) and adults (15+) by sex across the entire range of study (2009 to 2017). The model used in the analysis that includes prior completeness π_{k,t,a^*} ('Completeness') is shown compared to a model without any prior information on completeness ('Standard'). Each point represents the median of the draws of the raking factor, the bar represents 2.5th and 97.5th quantile of the draws, and the density curve represents the relative frequency of the draws. A raking factor closer to 1 (dotted line) indicates better alignment between model results and GBD estimates.

Figure S9: Model alignment with GBD, Mexico

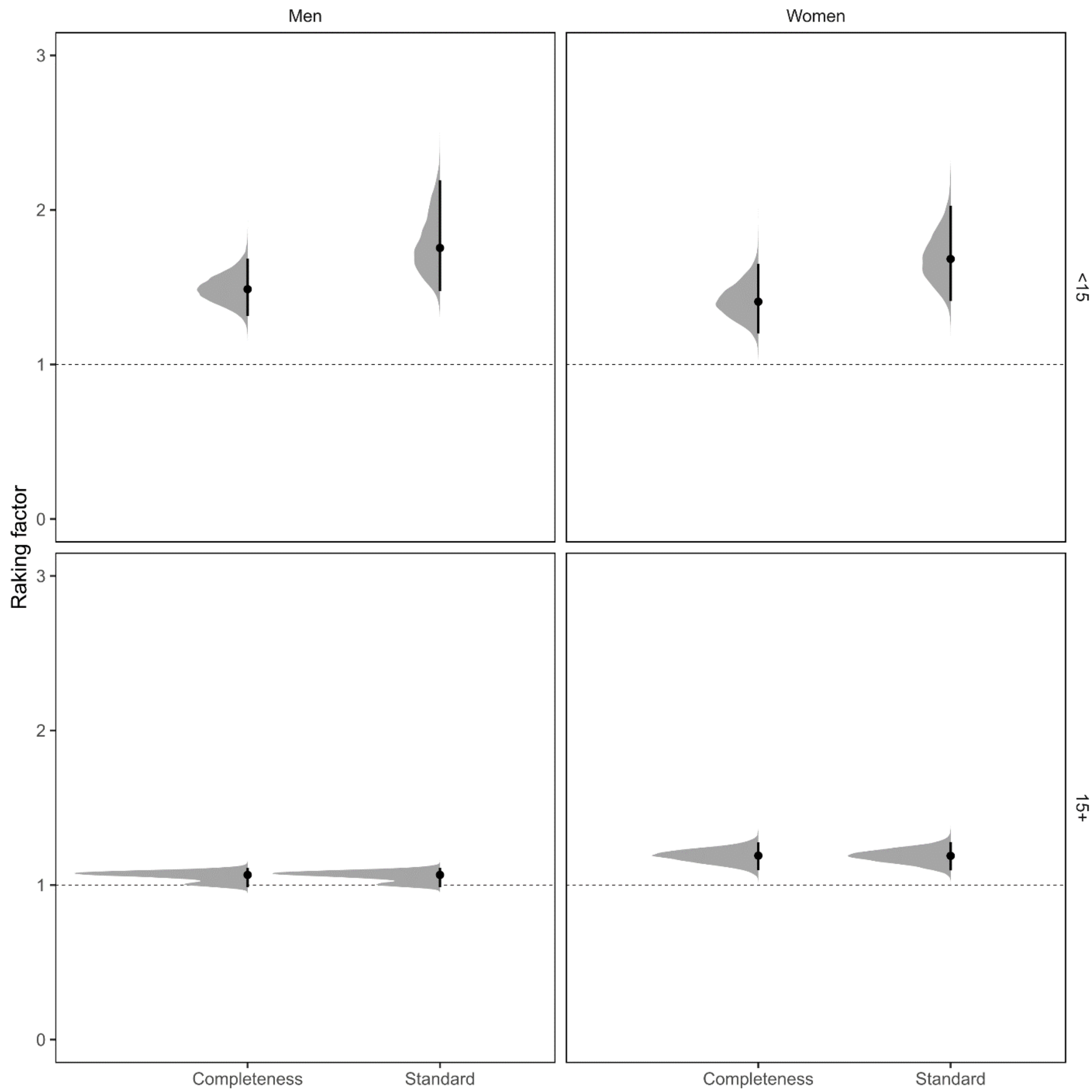

Figure S9: Model alignment with GBD, Mexico. Comparison of the annual ratio of national HIV mortality from GBD and 1,000 draws of annual national HIV mortality in children under-15 (<15) and adults (15+) by sex across the entire range of study (2000 to 2017). The model used in the analysis that includes prior completeness π_{k,t,a^*} ('Completeness') is shown compared to a model without any prior information on completeness ('Standard'). Each point represents the median of the draws of the raking factor, the bar represents 2.5th and 97.5th quantile of the draws, and the density curve represents the relative frequency of the draws. A raking factor closer to 1 (dotted line) indicates better alignment between model results and GBD estimates.

Figure S10: Mean and uncertainty in estimated HIV mortality in Brazil, 2017

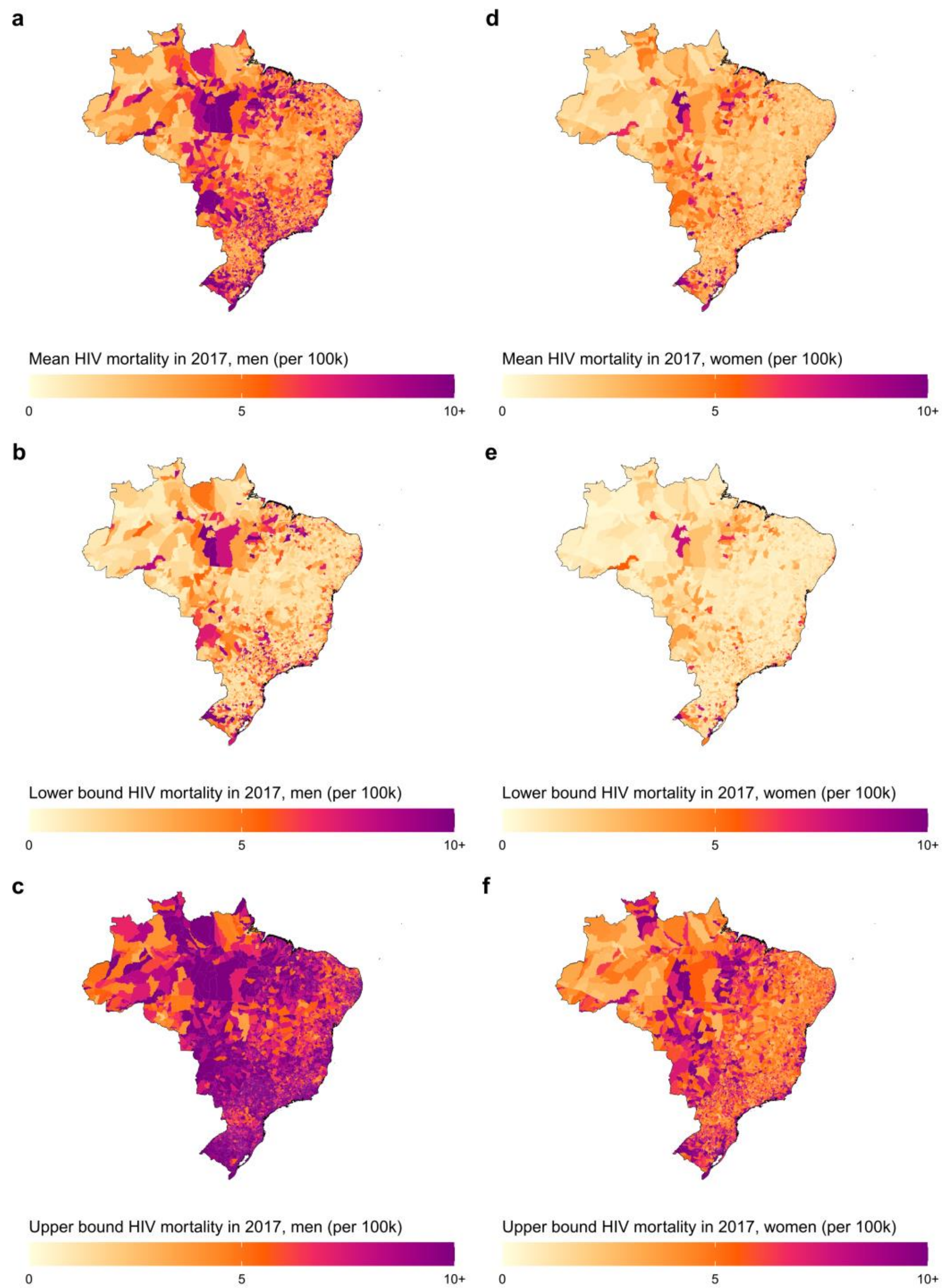

Figure S10: Mean and uncertainty in estimated HIV mortality in Brazil, 2017. Estimated HIV mortality at the municipality level in 2017 in Brazil among men (**a-c**) and women (**d-f**). Mean estimates and lower and upper bounds of the 95% uncertainty intervals are shown in the top, middle, and bottom column, respectively.

Figure S11: Mean and uncertainty in estimated HIV mortality in Colombia, 2017

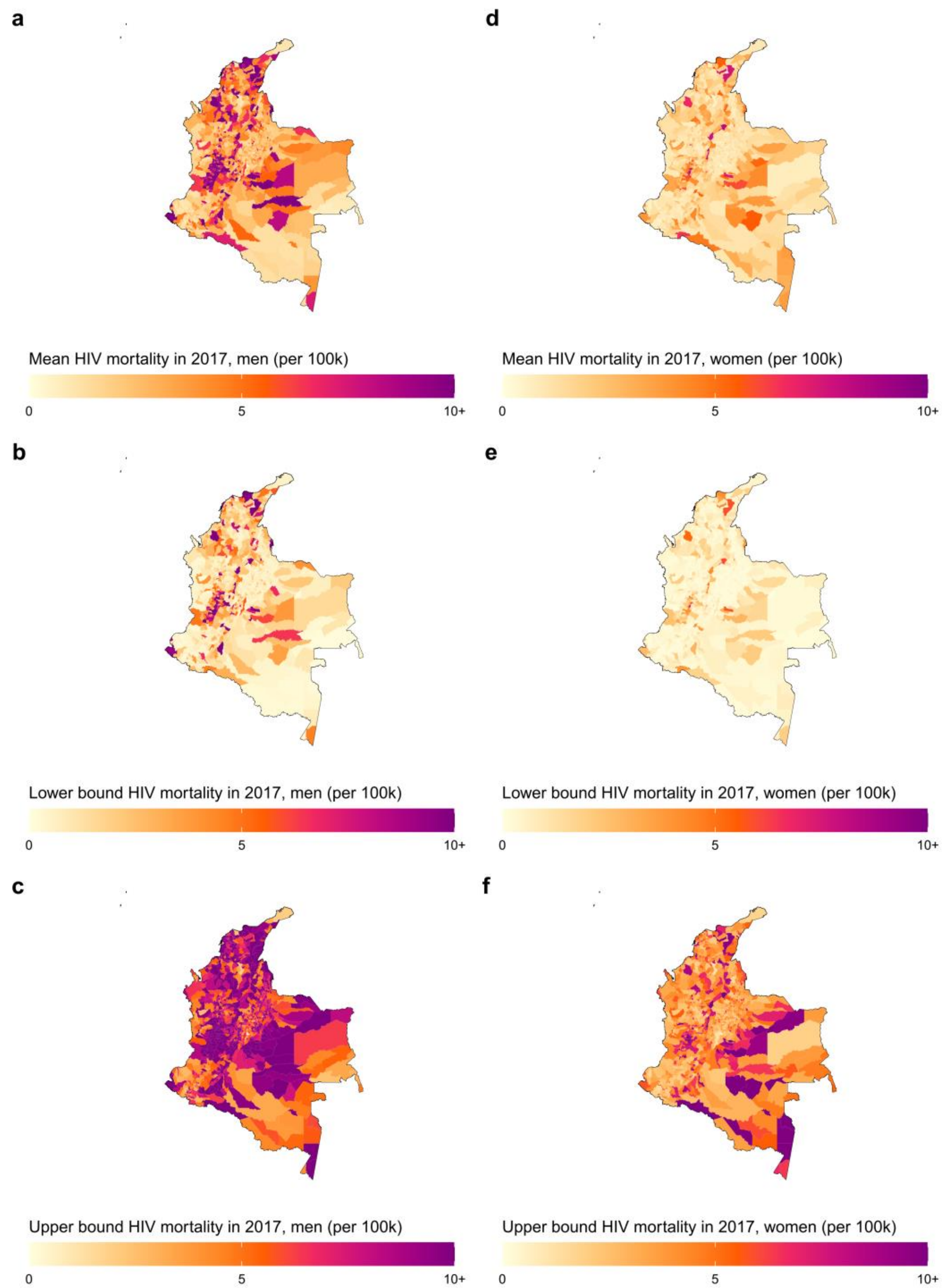

Figure S11: Mean and uncertainty in estimated HIV mortality in Colombia, 2017. Estimated HIV mortality at the municipality level in 2017 in Colombia among men (**a**-**c**) and women (**d**-**f**). Mean estimates and lower and upper bounds of the 95% uncertainty intervals are shown in the top, middle, and bottom column, respectively.

Figure S12: Mean and uncertainty in estimated HIV mortality in Costa Rica, 2016

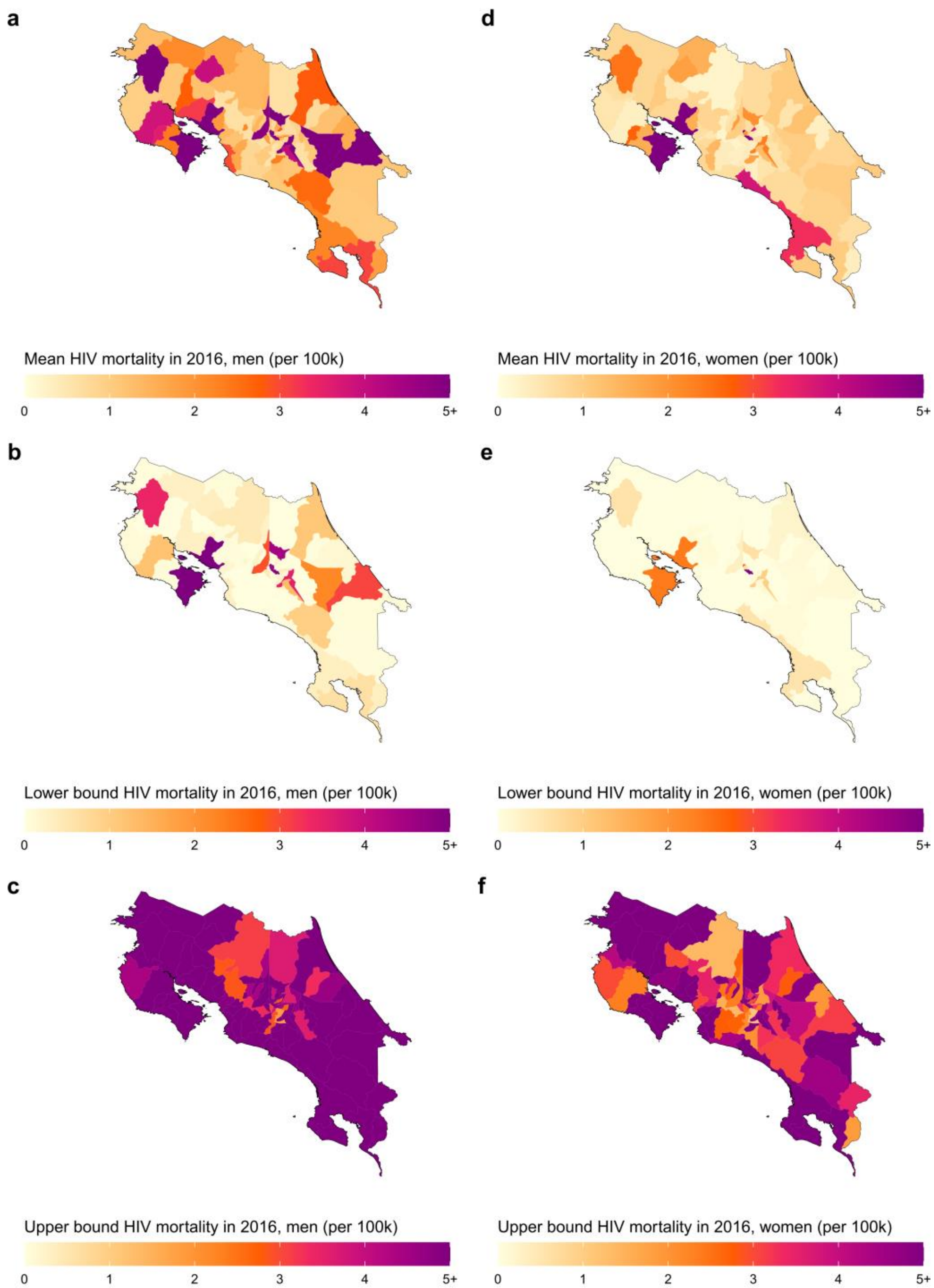

Figure S12: Mean and uncertainty in estimated HIV mortality in Costa Rica, 2016. Estimated HIV mortality at the canton level in 2016 in Costa Rica among men (**a-c**) and women (**d-f**). Mean estimates and lower and upper bounds of the 95% uncertainty intervals are shown in the top, middle, and bottom column, respectively.

Figure S13: Mean and uncertainty in estimated HIV mortality in Ecuador, 2014

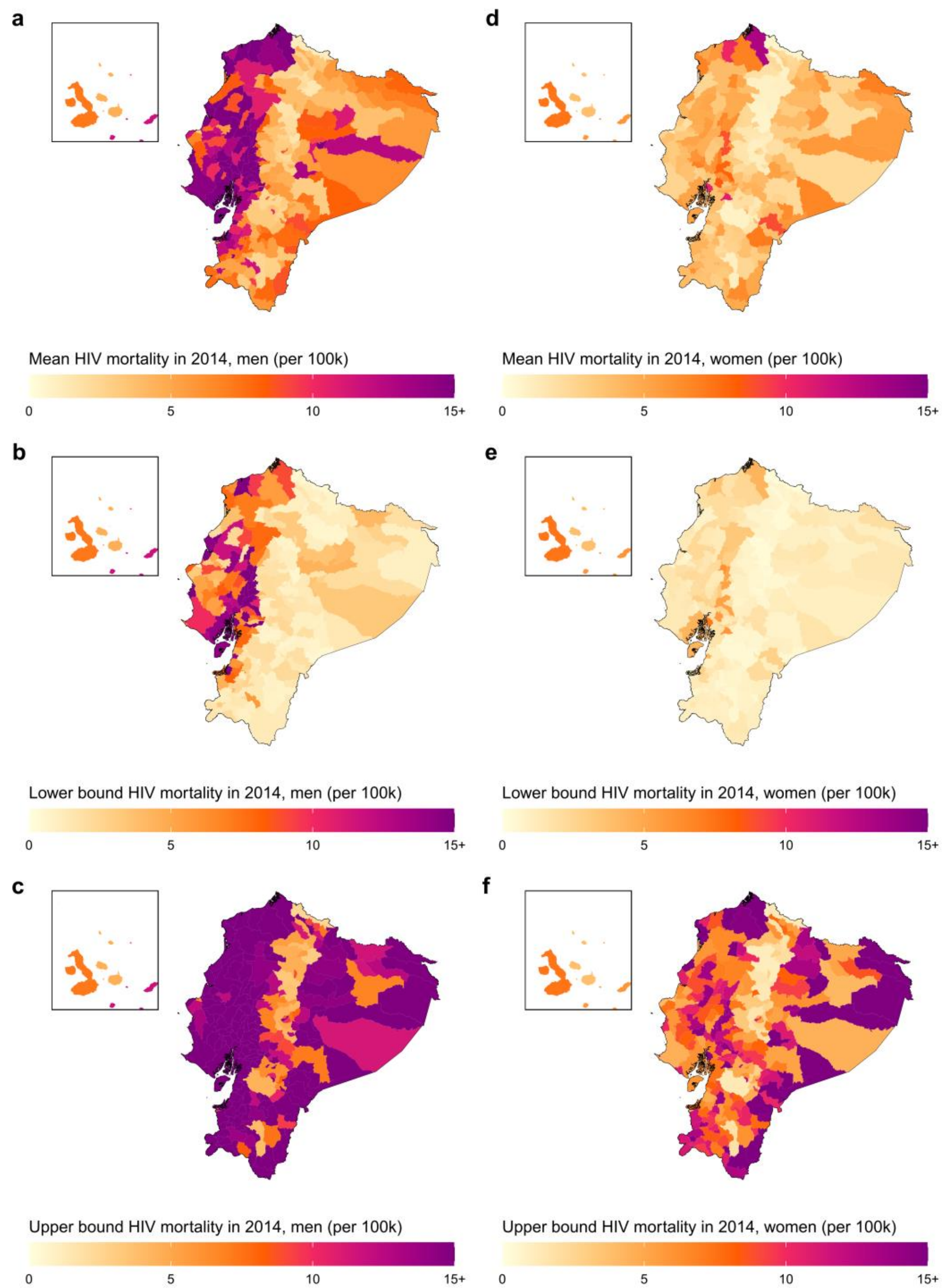

Figure S13: Mean and uncertainty in estimated HIV mortality in Ecuador, 2014. Estimated HIV mortality at the canton level in 2014 in Ecuador among men (**a-c**) and women (**d-f**). Mean estimates and lower and upper bounds of the 95% uncertainty intervals are shown in the top, middle, and bottom column, respectively.

Figure S14: Mean and uncertainty in estimated HIV mortality in Guatemala, 2017

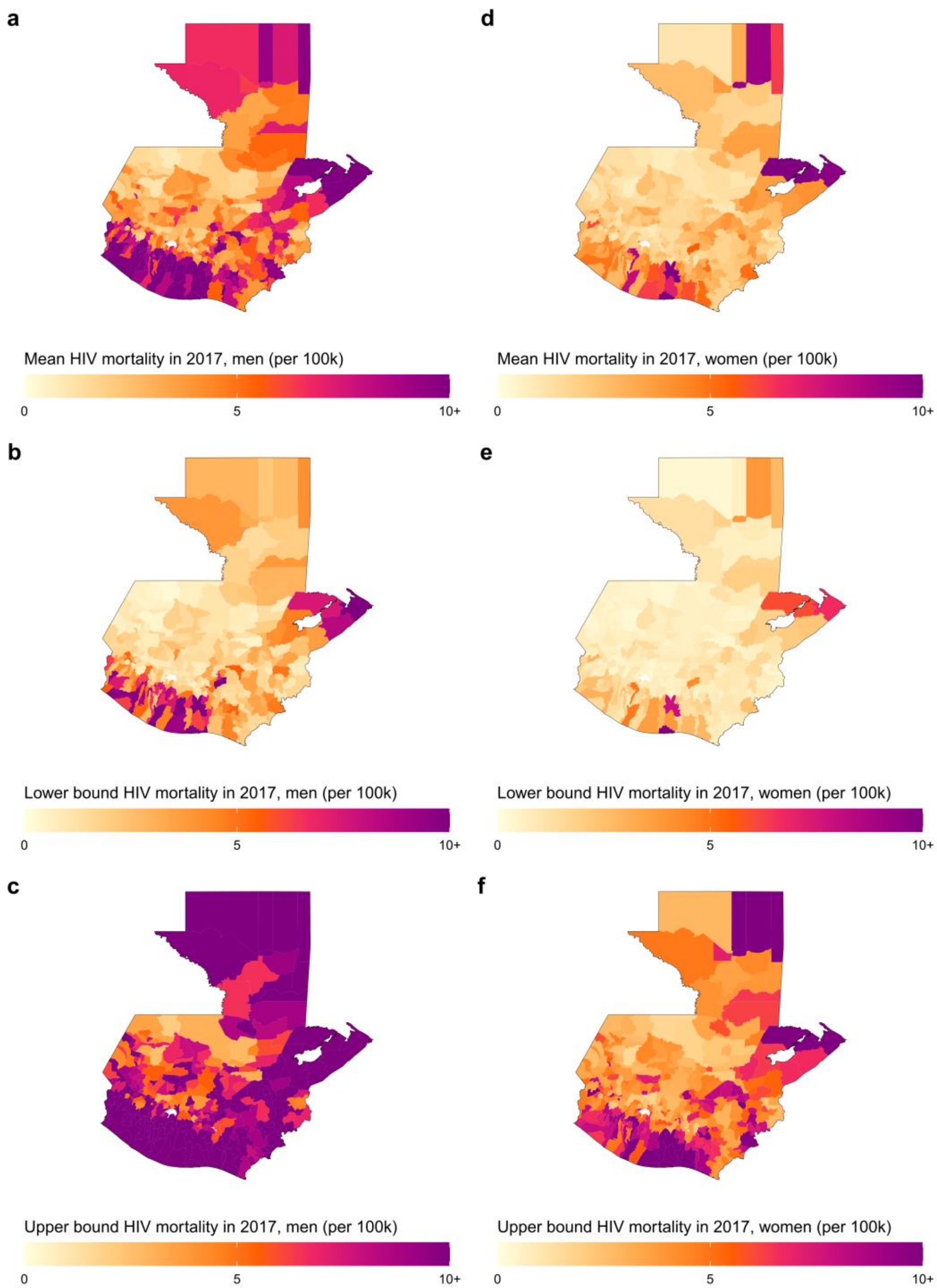

Figure S14: Mean and uncertainty in estimated HIV mortality in Guatemala, 2017. Estimated HIV mortality at the municipality level in 2017 in Guatemala among men (**a-c**) and women (**d-f**). Mean estimates and lower and upper bounds of the 95% uncertainty intervals are shown in the top, middle, and bottom column, respectively.

Figure S15: Mean and uncertainty in estimated HIV mortality in Mexico, 2017

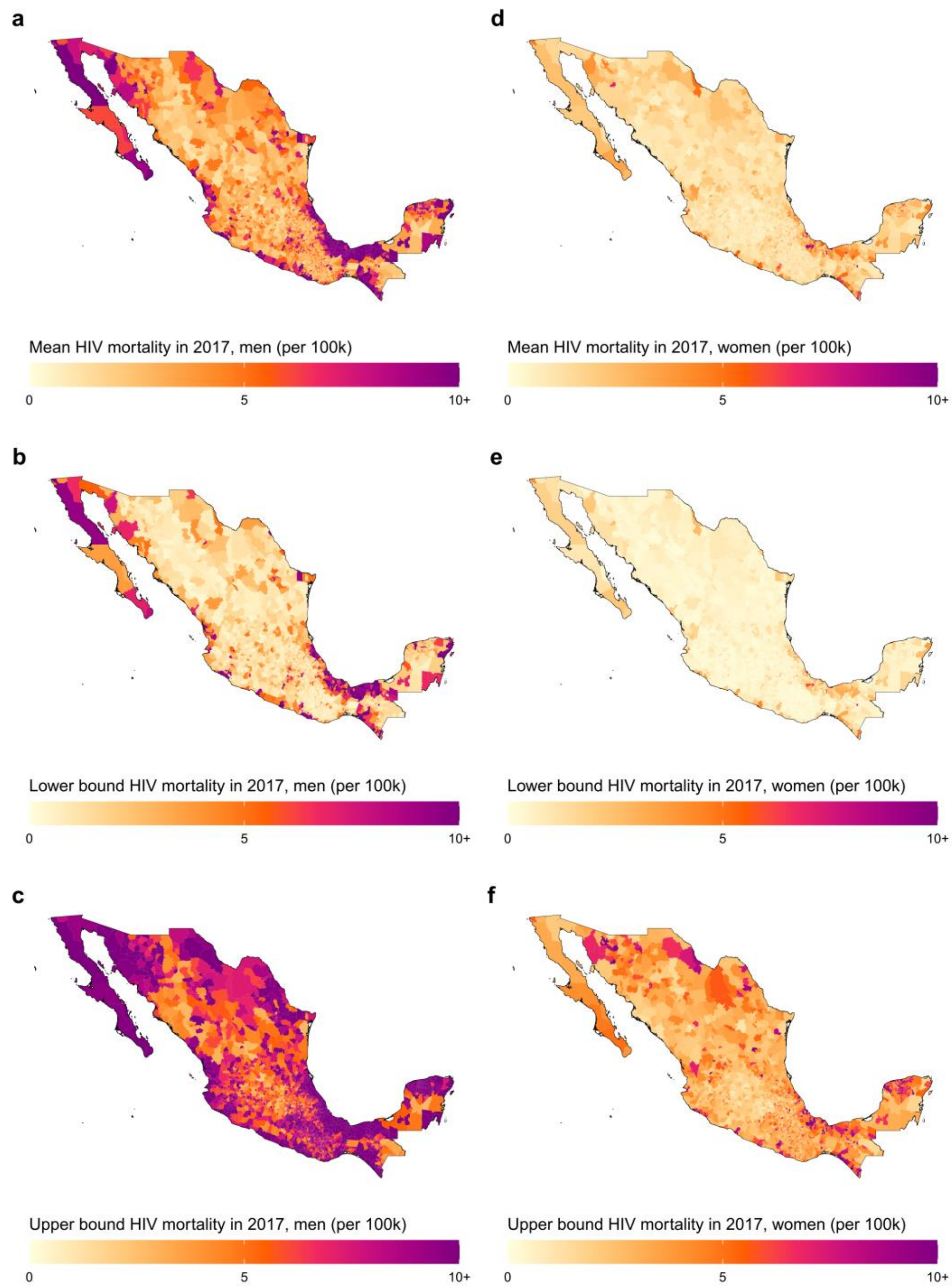

Figure S15: Mean and uncertainty in estimated HIV mortality in Mexico, 2017. Estimated HIV mortality at the municipality level in 2017 in Mexico among men (**a**-**c**) and women (**d**-**f**). Mean estimates and lower and upper bounds of the 95% uncertainty intervals are shown in the top, middle, and bottom column, respectively.

Figure S16: Estimated HIV mortality in Brazil by age group, 2017

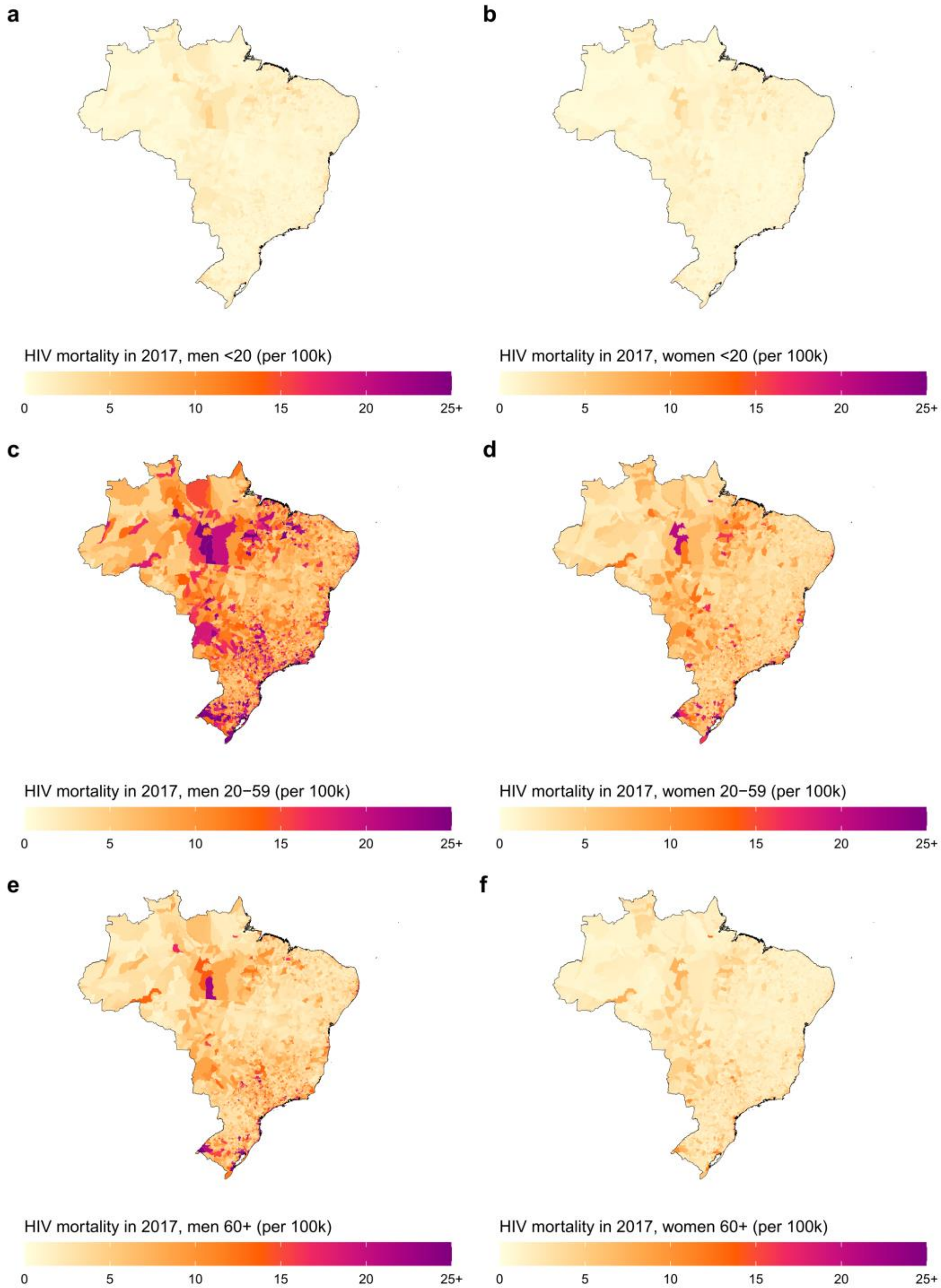

Figure S16: Estimated HIV mortality in Brazil by age group, 2017. Estimated HIV mortality at the municipality level in 2017 in Brazil among men (**a**) and women (**b**) less than 20 years of age, among men (**c**) and women (**d**) between 20 and 59 years of age, and among men (**e**) and women (**f**) over 60 years of age.

Figure S17: Estimated HIV mortality in Colombia by age group, 2017

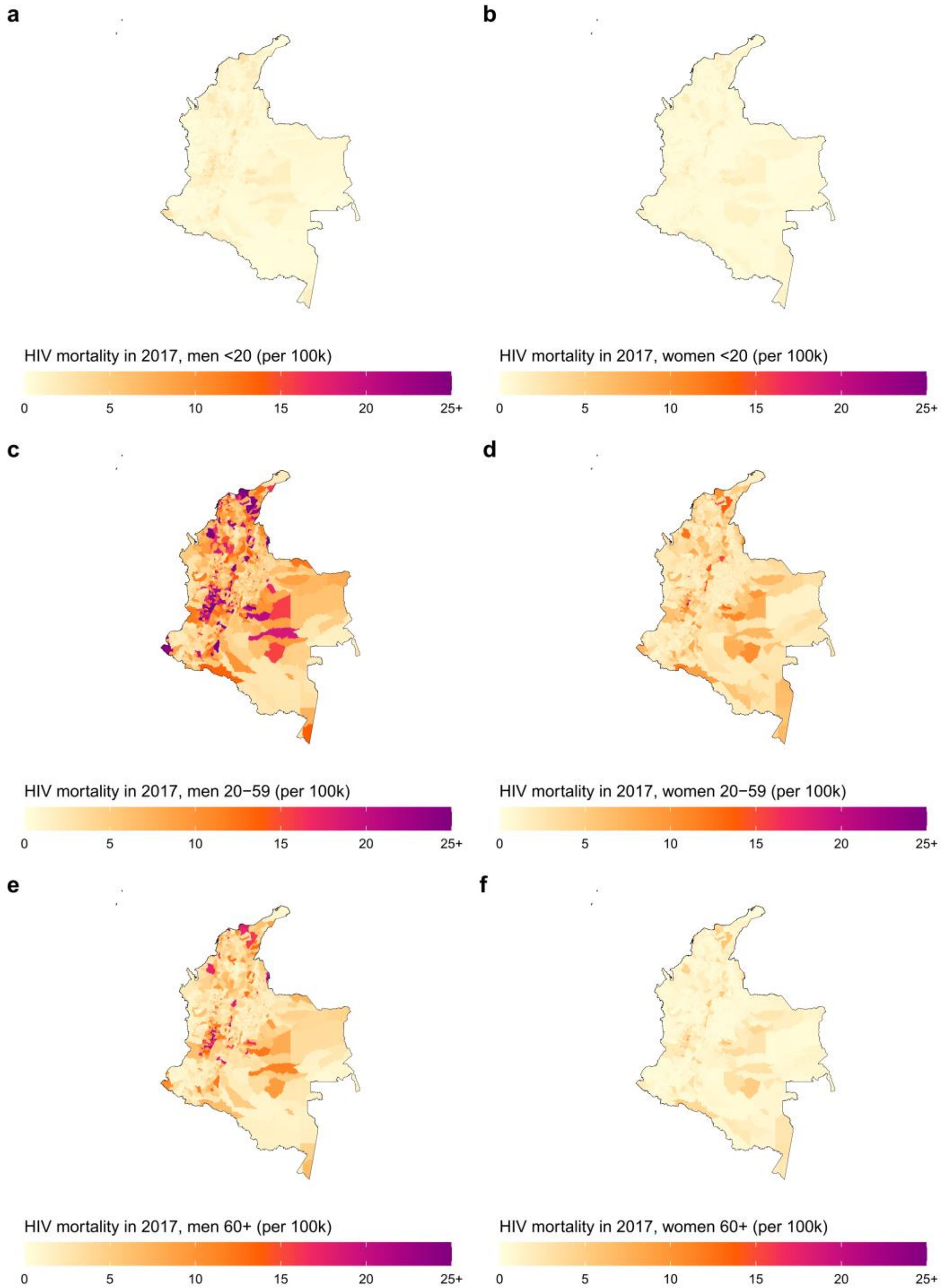

Figure S17: Estimated HIV mortality in Colombia by age group, 2017. Estimated HIV mortality at the municipality level in 2017 in Colombia among men (**a**) and women (**b**) less than 20 years of age, among men (**c**) and women (**d**) between 20 and 59 years of age, and among men (**e**) and women (**f**) over 60 years of age.

Figure S18: Estimated HIV mortality in Costa Rica by age group, 2016

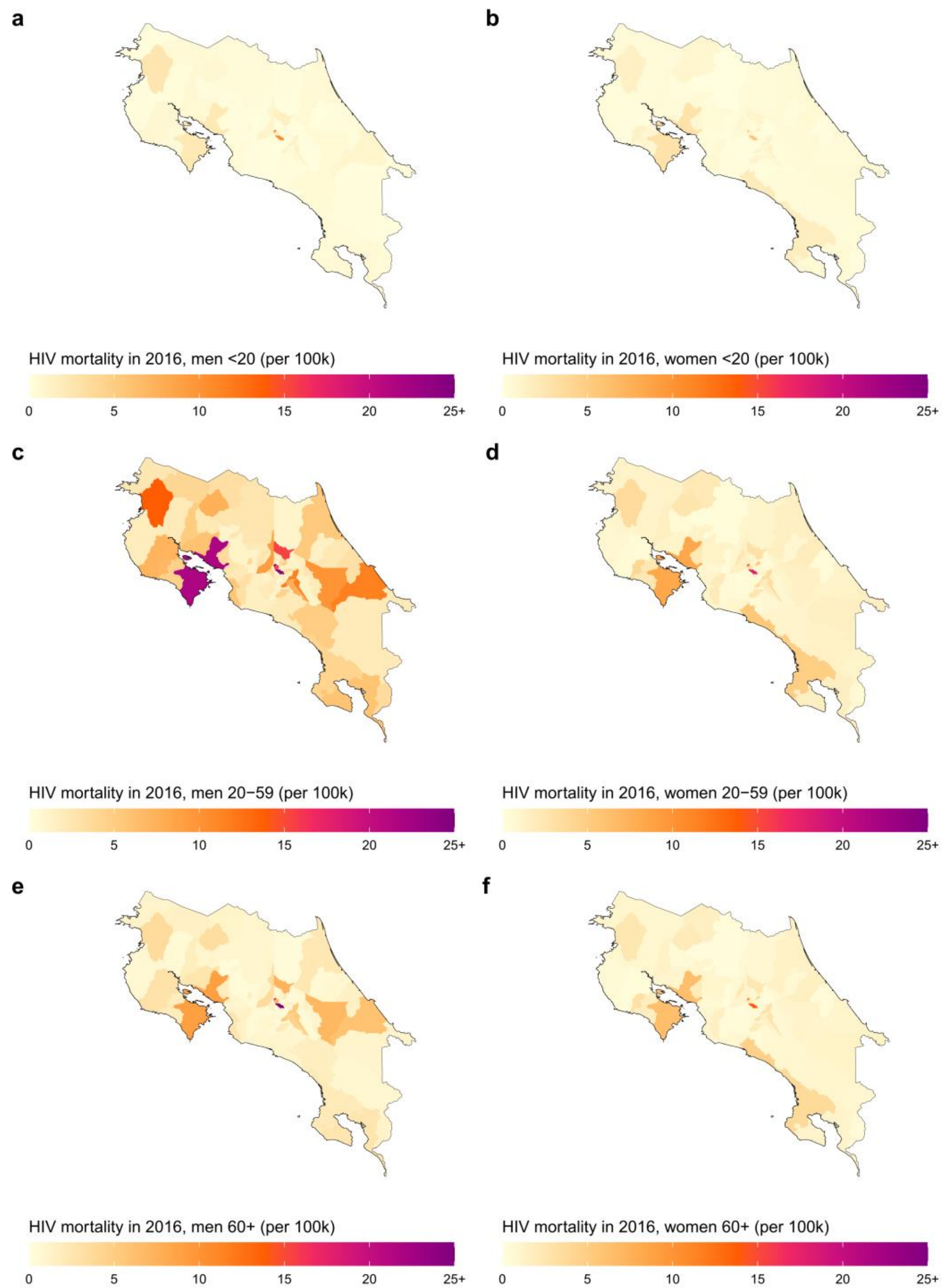

Figure S18: Estimated HIV mortality in Costa Rica by age group, 2016. Estimated HIV mortality at the canton level in 2016 in Costa Rica among men (**a**) and women (**b**) less than 20 years of age, among men (**c**) and women (**d**) between 20 and 59 years of age, and among men (**e**) and women (**f**) over 60 years of age.

Figure S19: Estimated HIV mortality in Ecuador by age group, 2014

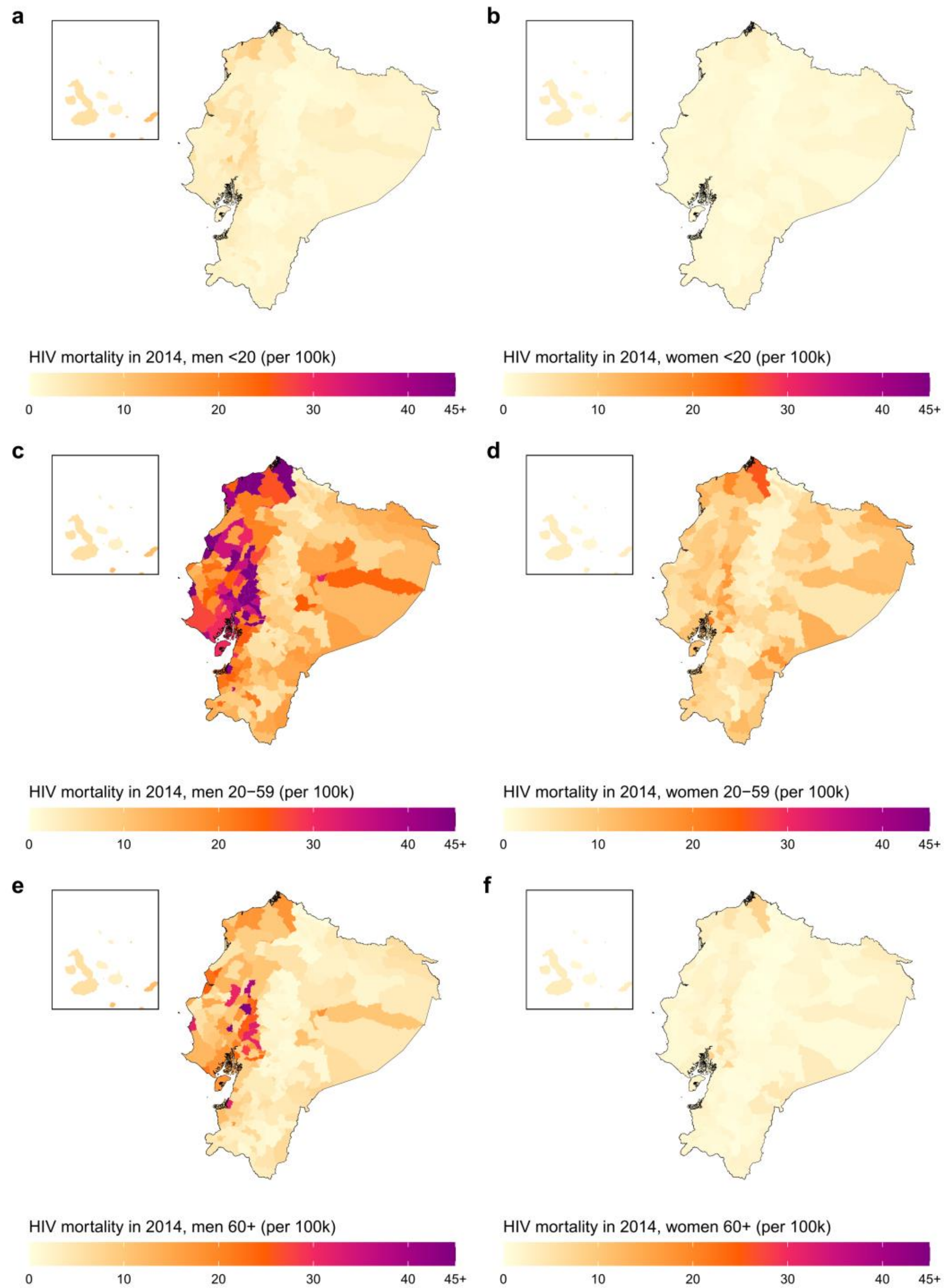

Figure S19: Estimated HIV mortality in Ecuador by age group, 2014. Estimated HIV mortality at the canton level in 2014 in Ecuador among men (**a**) and women (**b**) less than 20 years of age, among men (**c**) and women (**d**) between 20 and 59 years of age, and among men (**e**) and women (**f**) over 60 years of age.

Figure S20: Estimated HIV mortality in Guatemala by age group, 2017

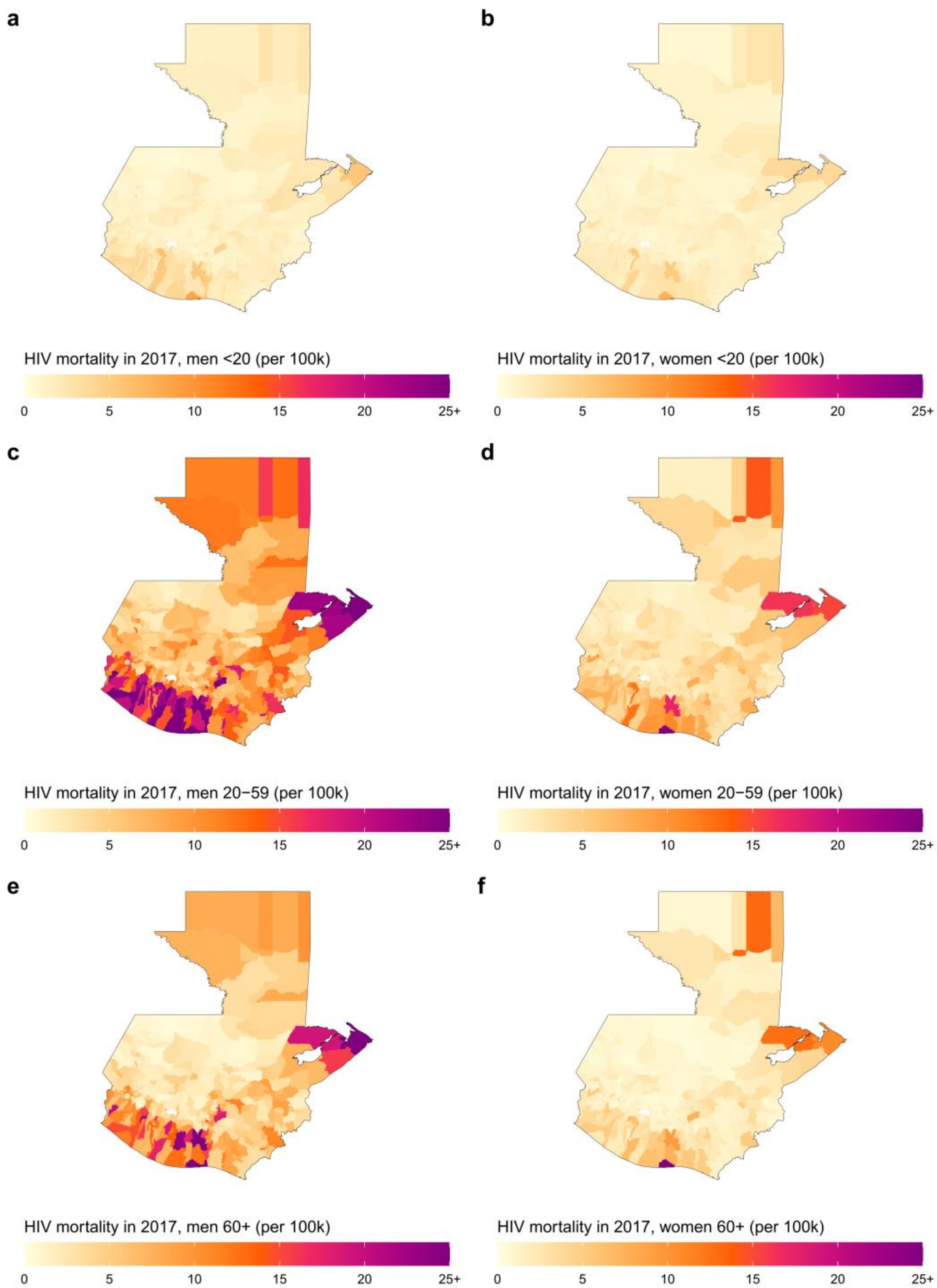

Figure S20: Estimated HIV mortality in Guatemala by age group, 2017. Estimated HIV mortality at the municipality level in 2017 in Guatemala among men (**a**) and women (**b**) less than 20 years of age, among men (**c**) and women (**d**) between 20 and 59 years of age, and among men (**e**) and women (**f**) over 60 years of age.

Figure S21: Estimated HIV mortality in Mexico by age group, 2017

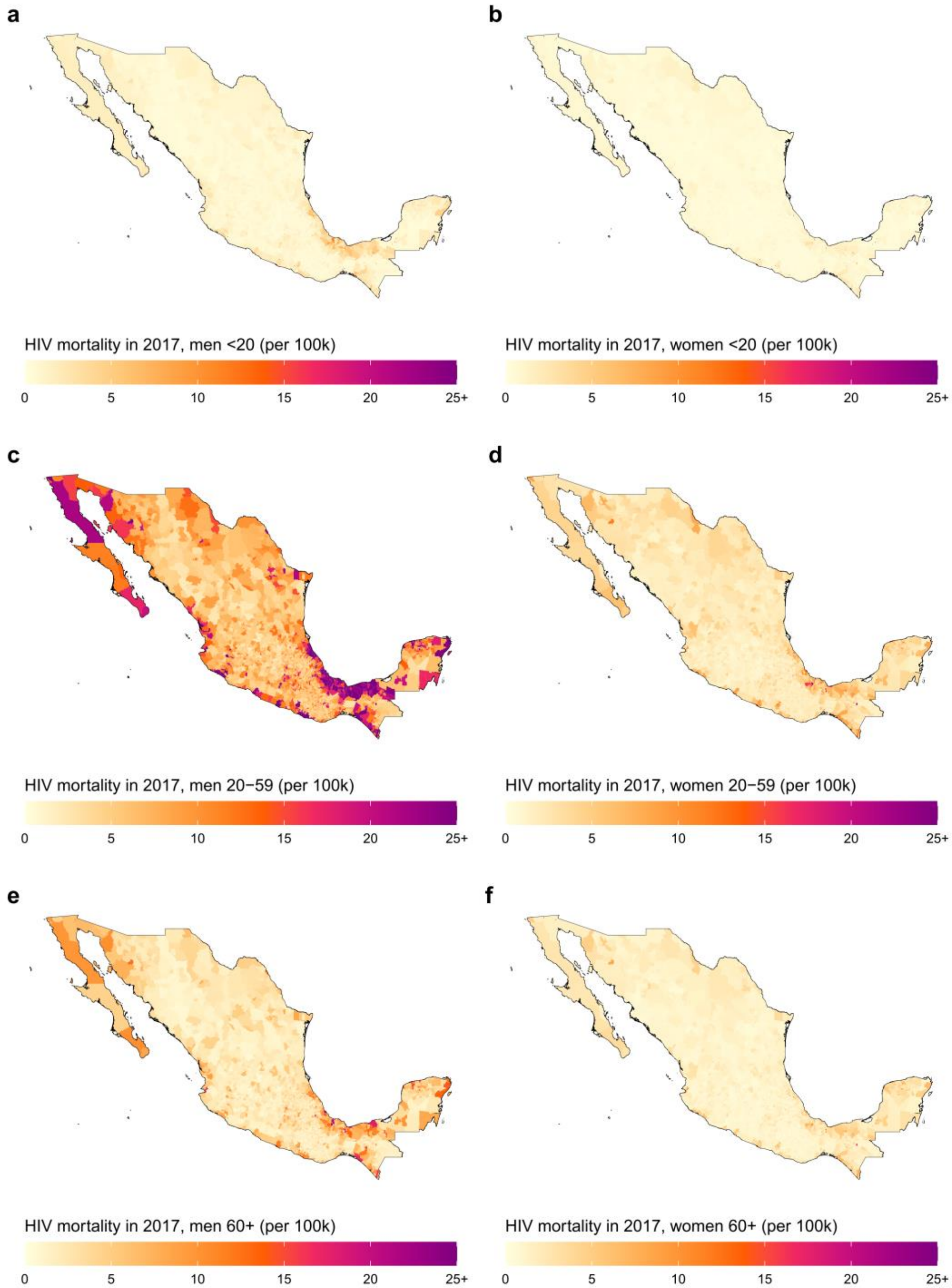

Figure S21: Estimated HIV mortality in Mexico by age group, 2017. Estimated HIV mortality at the municipality level in 2017 in Mexico among men (**a**) and women (**b**) less than 20 years of age, among men (**c**) and women (**d**) between 20 and 59 years of age, and among men (**e**) and women (**f**) over 60 years of age.

Supplemental tables

Table S1: Merged municipalities by country to form stable geographical units

Country	State	Group	Areas
Brazil	Para	1	Mojui dos Campos, Santarem
Brazil	Piaui	1	Altos, Pau D'Arco do Piaui
Brazil	Piaui	2	Aroeiras do Itaim, Picos
Brazil	Piaui	3	Nazaria, Teresina
Brazil	Rio Grande do Norte	1	Jundia, Varzea
Brazil	Alagoas	1	Coruripe, Jequia da Praia, Sao Miguel dos Campos
Brazil	Bahia	1	Barreiras, Luis Eduardo Magalhaes
Brazil	Bahia	2	Barrocas, Serrinha
Brazil	Espirito Santo	1	Colatina, Governador Lindenberg
Brazil	Rio de Janeiro	1	Mesquita, Nova Iguacu
Brazil	Santa Catarina	1	Criciuma, Balneario Rincao
Brazil	Santa Catarina	2	Laguna, Pescaria Brava
Brazil	Rio Grande do Sul	1	Acegua, Bage
Brazil	Rio Grande do Sul	2	Agua Santa, Caseiros, Ibiaca, Santa Cecilia do Sul, Tapejara
Brazil	Rio Grande do Sul	3	Almirante Tamandare do Sul, Carazinho
Brazil	Rio Grande do Sul	4	Arroio do Padre, Pelotas
Brazil	Rio Grande do Sul	5	Augusto Pestana, Boa Vista do Cadeado, Boa Vista do Incra, Bozano, Cruz Alta, Fortaleza dos Valos, Ijui
Brazil	Rio Grande do Sul	6	Barao de Cotegipe, Erechim, Jacutinga, Paulo Bento, Ponte Preta, Quatro Irmaos
Brazil	Rio Grande do Sul	7	Bento Goncalves, Pinto Bandeira, Pinto Bandeira
Brazil	Rio Grande do Sul	8	Caibate, Mato Queimado
Brazil	Rio Grande do Sul	9	Campinas do Sul, Cruzaltense
Brazil	Rio Grande do Sul	10	Canudos do Vale, Forquetinha, Lajeado, Progresso
Brazil	Rio Grande do Sul	11	Capao Bonito do Sul, Lagoa Vermelha
Brazil	Rio Grande do Sul	12	Capao do Cipo, Santiago, Sao Miguel das Missoes
Brazil	Rio Grande do Sul	13	Constantina, Novo Xingu
Brazil	Rio Grande do Sul	14	Coqueiro Baixo, Nova Brescia, Relvado
Brazil	Rio Grande do Sul	15	Coronel Pilar, Garibaldi, Roca Sales
Brazil	Rio Grande do Sul	16	Ernestina, Ibirapuita, Tio Hugo, Victor Graeff
Brazil	Rio Grande do Sul	17	Herval, Pedras Altas, Pinheiro Machado
Brazil	Rio Grande do Sul	18	Esmeralda, Pinhal da Serra

Brazil	Rio Grande do Sul	19	Espumoso, Jacuizinho, Salto do Jacui
Brazil	Rio Grande do Sul	20	Imigrante, Teutonia, Westfalia
Brazil	Rio Grande do Sul	21	Itati, Terra de Areia
Brazil	Rio Grande do Sul	22	Lagoa Bonita do Sul, Sobradinho
Brazil	Rio Grande do Sul	23	Marata, Montenegro, Salvador do Sul, Sao José do Sul
Brazil	Rio Grande do Sul	24	Palmeira das Missoes, Sao Pedro das Missoes
Brazil	Rio Grande do Sul	25	Rolador, Sao Luiz Gonzaga
Brazil	Rio Grande do Sul	26	Santa Margarida do Sul, Sao Gabriel
Brazil	Mato Grosso do Sul	1	Agua Clara, Camapua, Chapadao do Sul, Costa Rica, Figueirao, Paraiso das Aguas
Brazil	Mato Grosso	1	Agua Boa, Nova Nazare
Brazil	Mato Grosso	2	Alto Boa Vista, Bom Jesus do Araguaia, Cocalinho, Novo Santo Antonio, Ribeirao Cascalheira, Sao Felix do Araguaia, Serra Nova Dourada
Brazil	Mato Grosso	3	Aripuana, Colniza, Rondolandia
Brazil	Mato Grosso	4	Caceres, Curvelandia, Lambari D'Oeste, Mirassol d'Oeste
Brazil	Mato Grosso	5	Claudia, Itauba, Nova Santa Helena
Brazil	Mato Grosso	6	Conquista D'Oeste, Pontes e Lacerda, Vale de Sao Domingos
Brazil	Mato Grosso	7	Ipiranga do Norte, Itanhanga, Tapurah
Brazil	Mato Grosso	8	Nova Mutum, Santa Rita do Trivelato
Brazil	Mato Grosso	9	Novo Sao Joaquim, Santo Antonio do Leste
Brazil	Mato Grosso	10	Sao José do Xingu, Santa Cruz do Xingu
Brazil	Goias	1	Anapolis, Campo Limpo de Goias
Brazil	Goias	2	Ceres, Ipiranga de Goias
Brazil	Goias	3	Gameleira de Goias, Silvania
Brazil	Goias	4	Itaja, Lagoa Santa
Colombia	Bolivar	1	Norosi, Rio Viejo
Colombia	Cauca	1	Caloto, Guachene
Colombia	Cordoba	1	Montelibano, San José De Ure
Colombia	Cordoba	2	San Andres Sotavento, Tuchin
Colombia	Sucre	1	Covenas, Santiago De Tolu
Colombia	Amazonas	1	El Encanto, Puerto Alegria
Colombia	Guainia	1	Barranco Minas, Mapiripana
Costa Rica	Puntarenas	1	Aguirre, Aguirre
Ecuador	Los Rios	1	Quinsaloma, Ventanas
Ecuador	Pichincha, Santo Domingo De Los Tsachilas	1	Santo Domingo, Santo Domingo

Ecuador	Esmeraldas, Santo Domingo De Los Tsachilas, Zona No Delimitada	1	La Concordia, La Independencia, Plan Piloto, Quininde
Ecuador	Guayas, Santa Elena	1	Santa Elena, Santa Elena
Ecuador	Guayas, Santa Elena	2	La Libertad, La Libertad
Ecuador	Guayas, Santa Elena	3	Salinas, Salinas
Guatemala	Suchitepequez	1	Cuyotenango, San José La Maquina
Guatemala	San Marcos	1	La Blanca, Ocos
Guatemala	Huehuetenango	1	Concepcion Huista, Petatan
Guatemala	El Peten	1	La Libertad, Las Cruces
Guatemala	El Peten	2	Dolores, El Chal
Guatemala	Zacapa	1	San Jorge, Zacapa
Guatemala	Escuintla	1	La Gomera, Sipacate
Mexico	Guerrero	1	Azoyu, Cuajinicuilapa, Juchitan, Marquelia
Mexico	Guerrero	2	Chilapa de Alvarez, José Joaquin de Herrera
Mexico	Guerrero	3	Iliatenco, Malinaltepec, San Luis Acatlan
Mexico	Guerrero	4	Cochoapa el Grande, Metlatonoc
Mexico	Jalisco	1	Arandas, San Ignacio Cerro Gordo
Mexico	Mexico	1	Jaltenco, Tonanitla
Mexico	Mexico	2	San Felipe del Progreso, San José del Rincon
Mexico	Mexico	3	Luvianos, Tejupilco
Mexico	Quintana Roo	1	Bacalar, Othon P. Blanco
Mexico	Quintana Roo	2	Benito Juarez, Puerto Morelos
Mexico	Quintana Roo	3	Solidaridad, Tulum
Mexico	Veracruz de Ignacio de la Llave	1	Martinez de la Torre, San Rafael
Mexico	Veracruz de Ignacio de la Llave	2	Playa Vicente, Santiago Sochiapan
Mexico	Zacatecas	1	Santa Maria de la Paz, Teul de Gonzalez Ortega

*Group number differentiates between multiple merged areas that are within the same first-administrative level unit

459 Table S2: Vital Registration data

Country	Years	Reference	NID*
Brazil	2000–2017	Ministry of Health (Brazil). Brazil Mortality Information System – Deaths 2000-2017.Brasilia, Brazil: Ministry of Health (Brazil).	153037, 153038, 153039, 153040, 153041, 153042, 153043, 153044, 153045, 153046, 153048, 153049, 153050, 173779, 265226, 268267, 317728, 386735
Colombia	2000–2017	National Administrative Department of Statistics (DANE) (Colombia). Colombia Vital Statistics - Deaths 2000-2017. Bogotá, Colombia: National Administrative Department of Statistics (DANE) (Colombia).	397407, 397409, 397411, 397413, 397415, 397417, 397419, 397421, 65267, 65199, 57982, 265177, 265178, 265179, 265181, 265219, 265220, 396797
Costa Rica	2014–2016	National Institute of Statistics and Censuses (Costa Rica). Costa Rica Registered Deaths 2014-2016. San José, Costa Rica: National Institute of Statistics and Censuses (Costa Rica).	398942, 325066, 398943
Ecuador	2004–2014	National Institute of Statistics and Censuses (Ecuador). Ecuador General Deaths 2004-2014. Quito, Ecuador: National Institute of Statistics and Censuses (Ecuador).	343283, 343285, 343287, 343289, 256676, 256677, 256678, 256679, 256680, 256681, 325080
Guatemala	2009–2017	National Statistics Institute (Guatemala). Guatemala Vital Statistics 2009-2017. Guatemala City, Guatemala: National Statistics Institute (Guatemala).	336252, 336251, 336250, 240728, 240729, 240730, 286175, 335901, 398900
Mexico	2000–2017	National Institute of Statistics and Geography (INEGI) (Mexico). Mexico Vital Registration - Deaths 2000-2016.	116138, 116139, 116140, 116141, 116142, 116143, 116144, 116145, 116146, 93775, 116147, 107113, 124425, 157617, 240409, 281783,

			325345, 386753

*NID = Data source unique identifier in the Global Health Data Exchange (http://ghdx.healthdata.org/). Additional information about each data sources is available via the GHDx, including information about the data provider and links to where the data can be accessed or requested (where available). NIDs can be entered in the search bar to retrieve the record for a particular source.

Table S3: Covariate data sources

Covariate	Temporal resolution	Source	Reference	NID*
Population Density	2000–2017	WorldPop	Geography and Environmental Science, University of Southampton, WorldPop. Age and Sex Structures, Global Per Country 2000-2020. Southampton, United Kingdom: WorldPop, 2018.	420764
Nighttime lights	2000–2013	NOAA DMSP	National Oceanic and Atmospheric Administration (NOAA) (United States), United States Air Force (USAF). DMSP-OLS Nighttime Lights Time Series, V4. United States of America: National Oceanic and Atmospheric Administration (NOAA) (United States).	418630
Travel time to the nearest settlement > 50,000 inhabitants	None	Malaria Atlas Project, Big Data Institute, Nuffield Department of Medicine, University of Oxford	Nelson A, Joint Research Centre of the European Commission. Estimated travel time to the nearest city of 50,000 or more people in year 2000. Ispra, Italy: Global Environment Monitoring Unit, Joint Research Centre of the European Commission, 2008.	316680
Urbanicity	2000–2015	European Commission/ GHS	Pesaresi, Martino; Freire, Sergio (2016): GHS settlement grid, following the REGIO model 2014 in application to GHSL Landsat and CIESIN GPW v4-multitemporal (1975-1990-2000-2015). European Commission, Joint Research Centre (JRC) [Dataset] PID: http://data.europa.eu/89h/jrc-ghsl-ghs_smod_pop_globe_r2016a	418851

*NID = Data source unique identifier in the Global Health Data Exchange (http://ghdx.healthdata.org/). Additional information about each data sources is available via the GHDx, including information about the data provider and links to where the data can be accessed or requested (where available). NIDs can be entered in the search bar to retrieve the record for a particular source.

Table S4: National HIV mortality rates among men and women

HIV/AIDS mortality (age-standardized rates per 100,000) among men and women in six Latin American countries in the first and latest year of study						
Country	HIV mortality rate, (95% UI)*					
	Men		Women		Both Sexes	
	First Year	Latest Year	First Year	Latest Year	First Year	Latest Year
Brazil	11.7 (11.4-11.9)	8.7 (8.5-8.9)	5.3 (5.1-5.4)	4.5 (4.4-4.6)	8.4 (8.2-8.6)	6.5 (6.4-6.7)
Colombia	9.8 (9.3-10.2)	7.8 (7.5-8.1)	2.1 (1.9-2.3)	2.5 (2.3-2.7)	5.8 (5.5-6.1)	5.0 (4.8-5.3)
Costa Rica	6 (5.1-7.1)	4.9 (4.2-5.8)	1.9 (1.4-2.7)	1.5 (1.0-2.3)	3.9 (3.2-4.7)	3.2 (2.5-3.9)
Ecuador	8.5 (7.8-9.2)	10.9 (10.1-11.7)	2.1 (1.8-2.4)	3.4 (3-3.8)	5.2 (4.7-5.7)	7.0 (6.5-7.6)
Guatemala	10.8 (9.9-11.7)	6.8 (6.2-7.4)	4.1 (3.7-4.6)	2.8 (2.4-3.1)	7.2 (6.5-7.9)	4.6 (4.1-5.1)
Mexico	9 (8.8-9.3)	6.9 (6.7-7.1)	2.0 (1.9-2.1)	1.9 (1.8-2)	5.4 (5.2-5.5)	4.3 (4.1-4.4)

*UI = 95% uncertainty intervals